

3.0 RESULTS

The studies in REFLEX cover a wide range of frequencies within the spectrum of electromagnetic fields (EMF). Based on the assumption that possible biological effects may be generated by EMF in a different way dependent on their frequencies the results of the REFLEX project are reported separately for extremely low frequency electromagnetic fields (ELF-EMF) and radio frequency electromagnetic fields (RF-EMF).

3.1 Results in ELF-EMF research

3.1.1 Genotoxic effects

3.1.1.1 Human fibroblasts, lymphocytes, monocytes, melanocytes and muscle cells and granulosa cells of rats (Participant 3)

Intermittent ELF-EMF exposure, but not continuous ELF-EMF exposure induced DNA strand breaks in human fibroblasts.

In the first set of experiments fibroblasts were continuously exposed to ELF-EMF at 1000 μ T for 24h. In these experiments significant differences in DNA-breaks between exposed and sham-exposed cells were observed neither with the alkaline nor with the neutral Comet assay. As Nordenson et al. (1994) reported positive genotoxic effects applying intermittent field exposure, our next experiments concentrated on exposures at different intermittence conditions. Intermittence of 5 min on/5 min off and 15 min on/15 min off revealed an increase of DNA-breaks in both, the alkaline and the neutral Comet assay, compared to sham-exposed cells, whereas at 5 min on field/25 min off field did not enhance the frequency of DNA-breaks (Tables 2, 3).

Table 2. Mean values of alkaline Comet tailfactors at different exposure conditions (n = 2), cell strain IH-9

Alkaline Comet Assay - different exposure conditions				
	exposed		sham	
	Comet tailfactor %	\pm SD [#]	Comet tailfactor %	\pm SD [#]
Continuous exposure (24h)	4.29	0.02	4.27	0,03
15'/15' on/off	6.47*	0.14	4.23	0.05
5'/5' on/off	6.98*	0,04	4.41	0.16
5'/10' on/off	7.47*	0.13	4.48	0.05
5'/15' on/off	6.68*	0.17	4.42	0.03
5'/20' on/off	5.90*	0.12	4.38	0.12
5'/25' on/off	4.27	0.04	4.23	0.03
1'/10' on/off	5.89*	0.19	4.21	0.14
3'/10' on/off	6.60*	0.06	4.19	0.22
10'/10' on/off	6.91*	0.07	4.24	0.07
15'/10' on/off	6.56*	0.15	4.11	0.08
25'/10' on/off	5.37*	0.05	4.21	0.04

[#] SD indicates standard deviation

* indicates significant differences (p < 0.05) exposed vs. sham

Table 3. Mean values of neutral Comet tailfactors at different exposure conditions (n = 2), cell strain IH-9

Neutral Comet Assay - different exposure conditions				
	exposed		sham	
	Comet tailfactor %	±SD [#]	Comet tailfactor %	±SD [#]
Continuous exposure (24h)	4.20	0.03	4.17	0.05
15/15' on/off	5.72*	0.01	4.25	0.04
5/5' on/off	6.09*	0.02	4.31	0.08
5/10' on/off	6.21*	0.01	4.35	0.07
5/15' on/off	5.66*	0.06	4.23	0-13
5/20' on/off	4.52	0.16	4.50	0.21
5/25' on/off	4.25	0.05	4.34	0.07
1/10' on/off	4.16	0.15	4.16	0.13
3/10' on/off	5.94*	0.05	4.20	0.06
10/10' on/off	6.19*	0.11	4.11	0.11
15/10' on/off	6.02*	0.03	4.21	0.10
25/10' on/off	5.44	0.01	4.15	0.01

[#]SD indicates standard deviation

* indicates significant differences (p < 0.05) exposed vs. sham

Based on these findings, we tried to find out the optimal exposure conditions for maximal effects on DNA strand break levels. We started with a fixed field-on time of 5 min and varied field-off times from 5 to 25 min. These experiments indicated that DNA strand break levels (SSB and DSB) culminated at an off-time of 10 min and reached control levels at extended off-times (Figure 7). Significant differences (p < 0.01) between exposed and sham-exposed cells were found at 5 min on/5 min off, 5 min on/10 min off, 5 min on/15 min off and 5 min on/20 min off intermittence for alkaline Comet assay and at 5 min on/5 min off, 5 min on/10 min off and 5 min on/15 min off intermittence for neutral Comet assay, but not at 5 min on/25 min off for both assays.

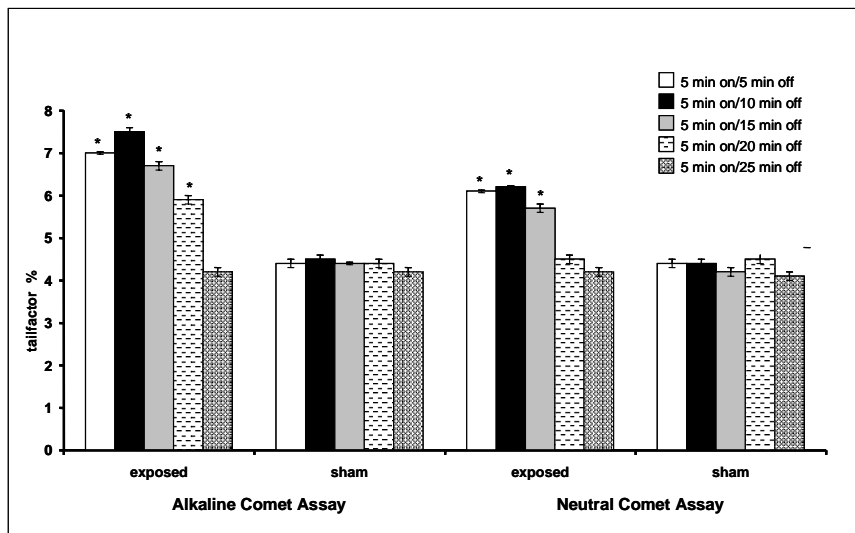


Figure 7. Alkaline and neutral Comet Assay tailfactors of ELF exposed fibroblasts (cell line IH-9, 50 Hz sinus, 24h, 1000 µT, intermittent) - variation of off-time. * p < 0.01 exposed versus sham-exposed

Subsequently, a fixed off-time of 10 min was chosen and on-times have been varied from 1 to 25 min. Again, the highest level of DNA strand breaks was obtained at an intermittence of 5 min on/10 min off

(Figure 8). Comet tailfactors of exposed and sham-exposed cells differed significantly at each on-time in alkaline Comet assay and at 3 to 15 min on in the neutral Comet assay. Solely the alkaline Comet tailfactors of 5 min on/10 min off, 5 min on/25 min off and 25 min on/10 min off-EMF exposed cells differed significantly to the other applied intermittence conditions. Since an intermittence of 5 min on/10 min off was able to induce the highest levels of DNA strand breaks in both alkaline and neutral Comet assay, further experiments were performed at 5 min on/10 min off.

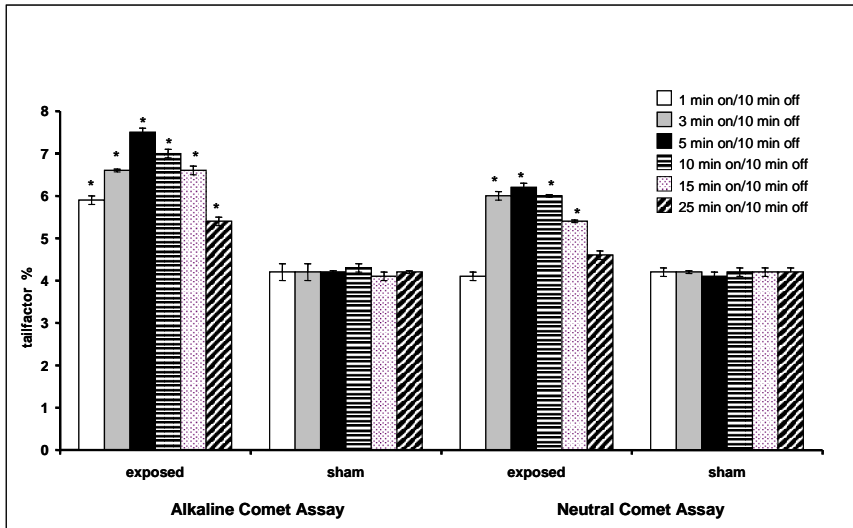


Figure 8. Alkaline and neutral Comet assay tailfactors of ELF exposed fibroblasts (cell line IH-9, 50 Hz sinus, 24 h, 1000 μ T, intermittent) - variation of on-time. * $p < 0.01$ exposed versus sham-exposed

ELF-EMF 50 Hz sinus generated a higher rate of DNA strand breaks in human fibroblasts than ELF-EMF powerline.

By comparing 50 Hz sinus to the 50 Hz powerline signal it was found out that at 50 Hz powerline Comet assay tailfactors were significantly lower than at 50 Hz sinusoidal (Figure 9). All further experiments in the ELF-EMF range were, therefore, carried out with 50 Hz sinus.

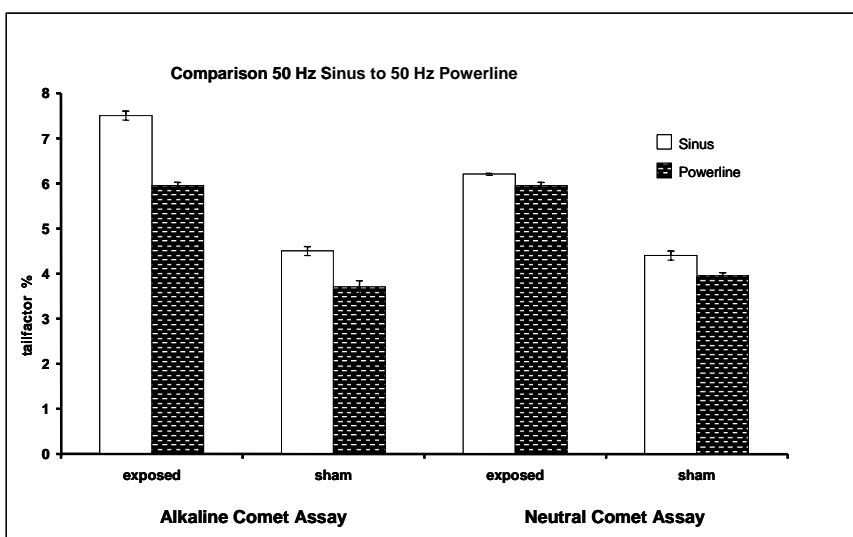


Figure 9. Alkaline and neutral Comet Assay tailfactors of ELF exposed fibroblasts (cell line IH-9, 24 h, 1000 μ T, intermittent)

Genotoxic effects were frequency dependent.

In order to investigate the frequency dependence of genotoxic effects of ELF-EMF (1 mT, 5 min on/10 min off) cultured human fibroblasts were exposed to different frequencies (3-550 Hz). Exposure time was set to 15 hours. Genotoxic effects were evaluated using the alkaline Comet assay. Figure 10 presents the tailfactors in exposed and sham exposed cells. Significant increases in DNA damage could be found at 3 Hz, 16 2/3 Hz, 30 Hz, 50 Hz, 300 Hz, and 550 Hz. Effects on strand break levels varied with the applied frequencies and could be ranked as follows: 50 Hz > 162/3 Hz > 3 Hz > 300 Hz > 550 Hz > 30 Hz. Quite obviously, the extent of induced DNA damage did not correlate with the applied frequency.

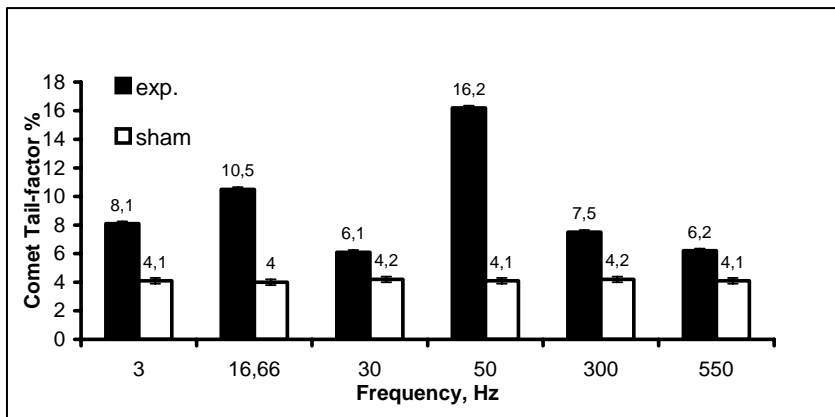


Figure 10. Alkaline Comet Assay tailfactors of ELF-EMF exposed and sham exposed fibroblasts (cell line ES-1, 15 hrs, 1000 μ T, intermittent) after variation of exposure frequency (3-550 Hz).

Increase in DNA strand breaks in human fibroblasts after ELF-EMF exposure was dependent on exposure time.

Alkaline and neutral Comet tailfactors increased with exposure time (1-24 hours, 1000 μ T, intermittent (5 min on/10 min off)), being largest at 15 hours (Figure 11). Comet assay levels declined thereafter, but did not return to basal levels.

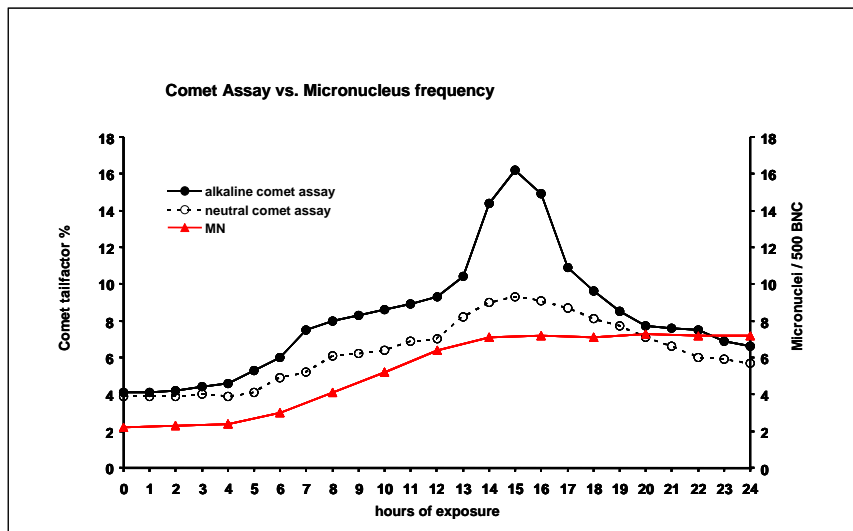


Figure 11. Influence of exposure time on formation of DNA single and double strand breaks and micronuclei in human fibroblasts (cell strain ES-1, 1 mT, 5 min on/10 min off cycles).

Increase in DNA strand breaks in human fibroblasts after ELF-EMF exposure was dependent on the age of the donors.

Fibroblasts from six healthy donors (ES1, male, 6 years old; AN2, female, 14 years old; IH9, female, 28 years old; KE1, male, 43 years old; HN3, female, 56 years old; WW3, male, 81 years old) revealed differences in response to ELF-EMF exposure (Table 4). Cells from older individuals exhibited a higher rate of single and double strand breaks and their break levels started to decline later than in cells from younger donors (Figures 12, 13).

Table 4. Alkaline and neutral Comet assay tailfactors of donors with different age (ES-1: 6, AN2: 14, IH9: 28, KE1: 43, HN3: 56, WW3: 81 years of age) - variation of exposure duration (basal-, maximum-, and end-levels)

	cell strain	hours exposure duration	Alkaline Comet Assay		Neutral Comet Assay	
			Comet tailfactor %	±SD [#]	Comet tailfactor %	±SD [#]
basal levels	ES1	0	4.112	0.018	3.901	0.006
	AN2	0	4.077	0.064	3.900	0.035
	IH9	0	4.223	0.047	4.161	0.148
	KE1	0	6.227	0.044	5.224	0.013
	HN3	0	6.802	0.018	6.313	0.064
	WW3	0	7.101	0.064	6.816	0.023
maximum levels	ES1	15	16.155	0.184	9.305	0.057
	AN2	15-16	16.501	0.004	9.394	0.134
	IH9	16	16.707	0.040	9.716	0.054
	KE1	18	17.300	0.064	10.462	0.277
	HN3	18-19	18.311	0.078	11.364	0.122
	WW3	19	18.517	0.069	12.822	0.076
and levels	ES1	24	6.611	0.017	5.742	0.023
	AN2	24	7.210	0.062	5.824	0.030
	IH9	24	7.511	0.017	6.127	0.054
	KE1	24	8.242	0.038	6.738	0.023
	HN3	24	8.718	0.008	6.761	0.006
	WW3	24	9.229	0.037	8.010	0.063

#SDstandard deviation

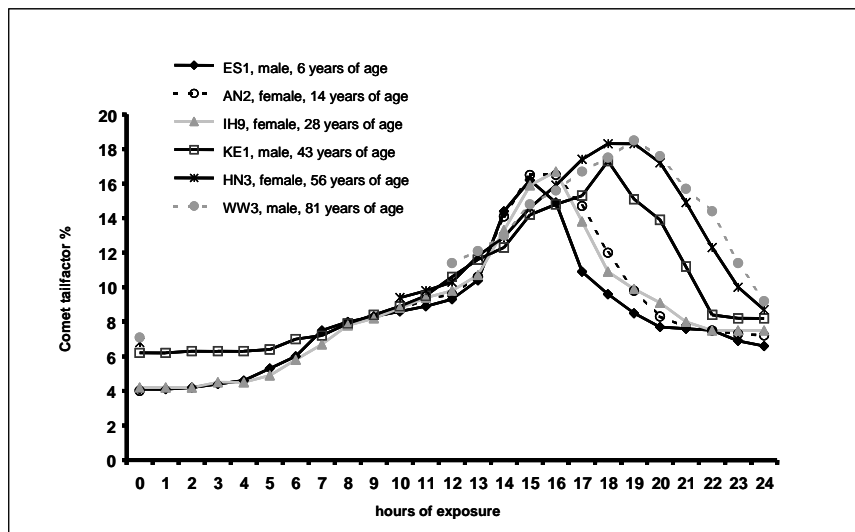


Figure 12. Alkaline Comet tailfactors of human diploid fibroblasts of donors with different years of age exposed to ELF-EMF (1 mT, intermittent 5 min on/10 min off) for 1-24 hours

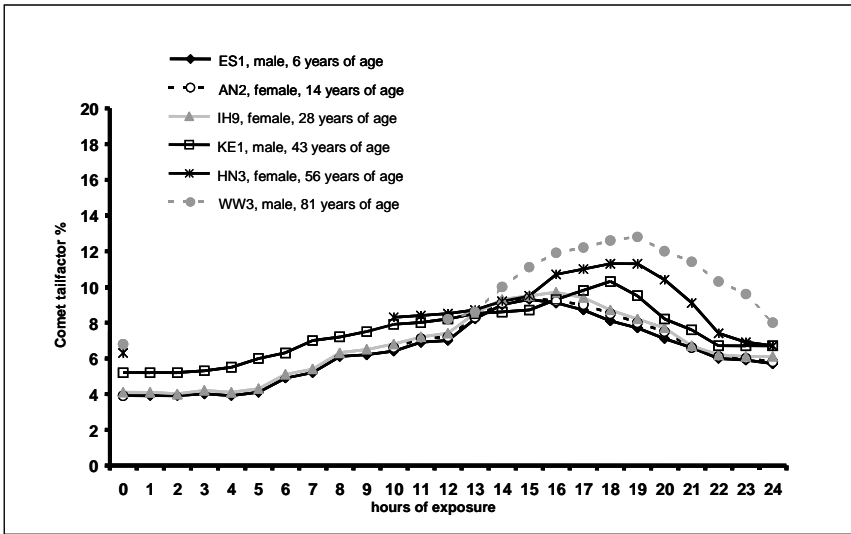


Figure 13. Neutral Comet tailfactors of human diploid fibroblasts of donors with different years of age exposed to ELF-EMF (1 mT, intermittent 5 min on/10 min off) for 1-24 hours

Increase in DNA strand breaks in human fibroblasts after ELF-EMF exposure was accompanied by a rise in micronuclei frequencies.

In addition, variation of exposure time from 2 to 24 hours revealed a time dependent increase in micronucleus frequencies. As shown in Figure 11, this increase became significant ($p < 0.05$) at 10 hours of ELF-EMF exposure. Thereafter, micronucleus frequencies reached a constant level, which was about 3-fold as compared to the basal levels (Figure 14).

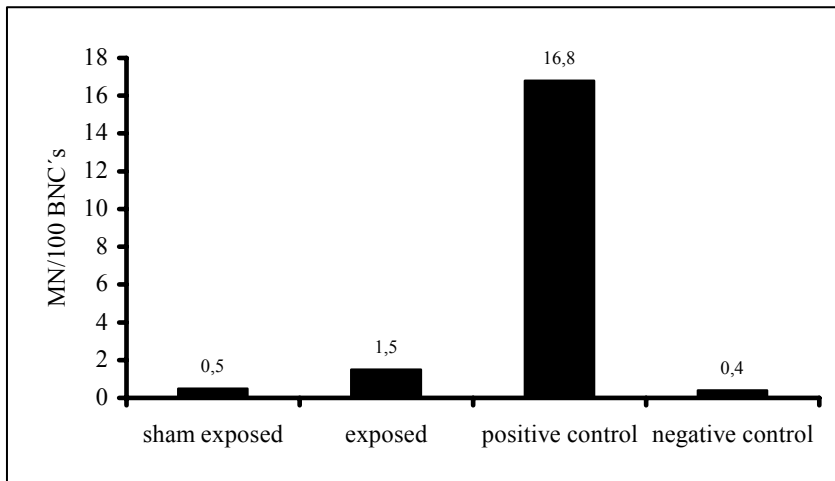


Figure 14. Micronucleus frequencies of ELF-EMF exposed (50 Hz, 1 mT, 15 h, 5 min on/10 min off) cultured human fibroblasts and controls (Vienna). Bleomycin 10 μ g/ml was used as a positive control.

ELF-EMF exposure did not diminish the number of fibroblasts in culture.

No differences in cell count between exposed and sham exposed cells at any exposure duration could be detected. Therefore, an elimination of cells by apoptosis and cell death during ELF-EMF exposure can probably be ruled out.

ELF-EMF exposure induced DNA strand breaks in human fibroblasts in a dose dependent way.

When magnetic flux density increased from 20 to 1,000 μT , a dose dependent rise in Comet assay tailfactors could be observed. At an exposure time of 24 hours a magnetic flux density as low as 70 μT produced significantly elevated ($p < 0.01$) alkaline and neutral Comet assay levels as compared to sham-exposed controls (Figure 13). At 15 hours of exposure genotoxic effects already occurred at 35 μT (Table 5, Figure 12). Using regression analysis, a significant correlation between Comet tailfactors and applied magnetic field (alkaline Comet assay: $r = 0.843$, $p = 0.004$; neutral Comet assay: $r = 0.908$, $p = 0.0007$), as well as between alkaline and neutral Comet assay could be found ($r = 0.974$, $p = 0.00001$).

Table 5. Mean values of alkaline and neutral Comet tailfactors at intermittent ELF exposure (5/10 on/off, 1000 μT , 24 h) ($n = 2$) dose response, cell line ES-1

μT magnetic flux density	Alkaline Comet Assay				Neutral Comet Assay			
	exposed		sham		exposed		sham	
	tailfactor %	$\pm\text{SD}^\#$	tailfactor %	$\pm\text{SD}^\#$	tailfactor %	$\pm\text{SD}^\#$	tailfactor %	$\pm\text{SD}^\#$
20	4.16	0.02	4.21	0.13	3.63	0.01	3.60	0.08
50	4.16	0.06	4.20	0.12	3.70	0.16	3.72	0.03
70	4.87*	0.03	4.28	0.02	3.99*	0.01	3.71	0.01
100	5.25*	0.06	4.28	0.05	4.32*	0.00	3.73	0.04
250	5.31*	0.02	4.25	0.07	4.24*	0.06	3.60	0.02
500	5.52*	0.01	4.22	0.01	4.48*	0.02	3.79	0.05
750	6.17*	0.08	4.26	0.11	5.08*	0.08	3.67	0.10
1000	6.50*	0.18	4.27	0.10	5.71*	0.01	3.79	0.16
2000	6.62	0.01	4.13	0.04	5.79*	0.05	3.70	0.01

SD indicates standard deviation
 • indicates significant differences ($p < 0.05$) exposed vs. sham

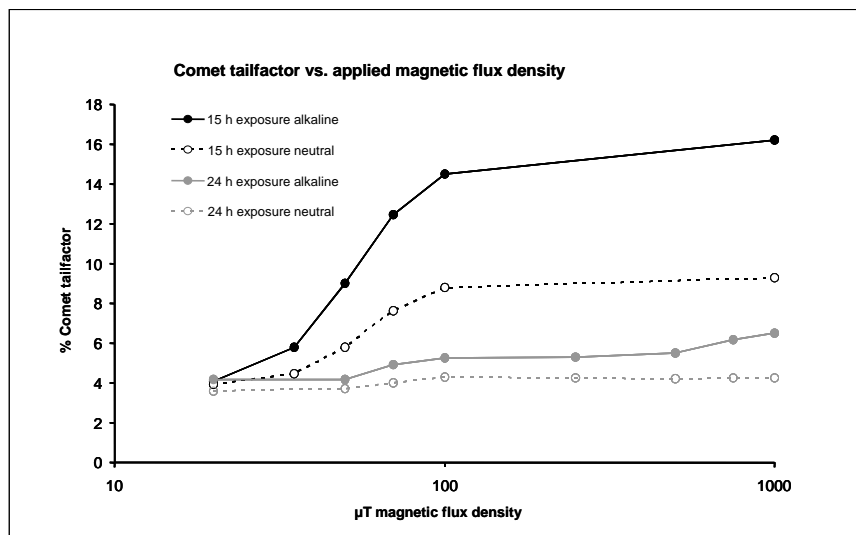


Figure 15. Dose dependent formation of DNA single and double strand breaks determined with Comet assay under alkaline and neutral conditions with cell strain ES-1 (exposure time 15 and 24 hours, 5 min on/10 min off cycles)

DNA strand breaks in human fibroblasts after ELF-EMF exposure were rapidly repaired.

After having demonstrated a time dependent relationship between alkaline and neutral Comet assay tailfactors and ELF-EMF exposure, the next aim was to find an explanation for the declining of the Comet assay levels after reaching the peak value. When exposure was terminated after 12 or 15 hours the Comet tailfactors returned to basal levels after a repair time of 7 to 9 hours (Figures 15, 16), comprising in a fast repair rate of DNA single strand breaks (< 1 hour) and a slow repair rate of DNA double strand breaks (> 7 hours). The marked Comet peak value between 12-17 hours disappeared when the Comet assay was performed at pH 12.1 instead of pH >13, thereby eliminating the cleavage of alkali labile sites in the DNA (Figure 18). The decline of Comet tailfactors after 15-20 hours of exposure could be prevented, when the cells were exposed in the presence of 10 µg/ml cycloheximide, an inhibitor of protein synthesis (Figure 18).

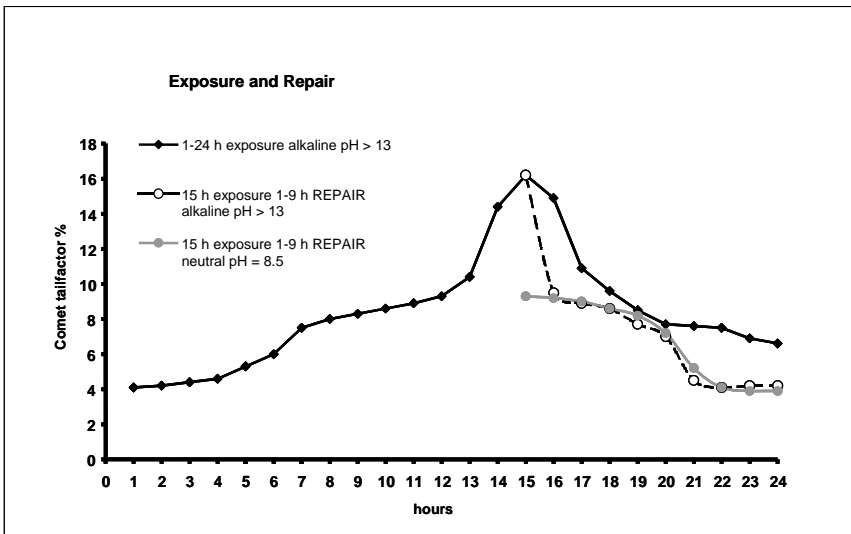


Figure 16. Repair kinetics of DNA single and double strand breaks in human fibroblasts (cell strain ES-1) after termination of ELF-EMF exposure (cell strain ES-1, 1 mT, 5 min on/10 min off cycles) using alkaline and neutral Comet assay - repair after 15 h ELF-EMF exposure

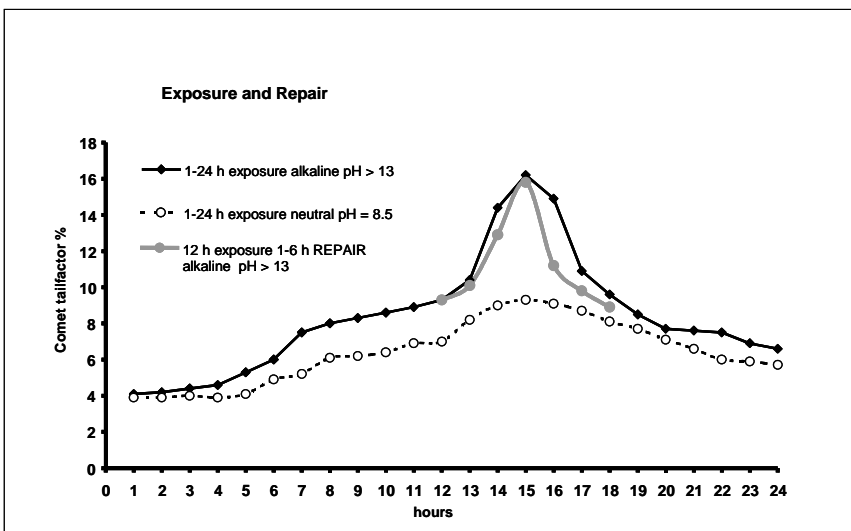


Figure 17. Repair kinetics of DNA single and double strand breaks in human fibroblasts (cell strain ES-1) after termination of ELF-EMF exposure (cell strain ES-1, 1 mT, 5 min on/10 min off cycles) using alkaline and neutral Comet assay - repair after 12 hours ELF-EMF exposure

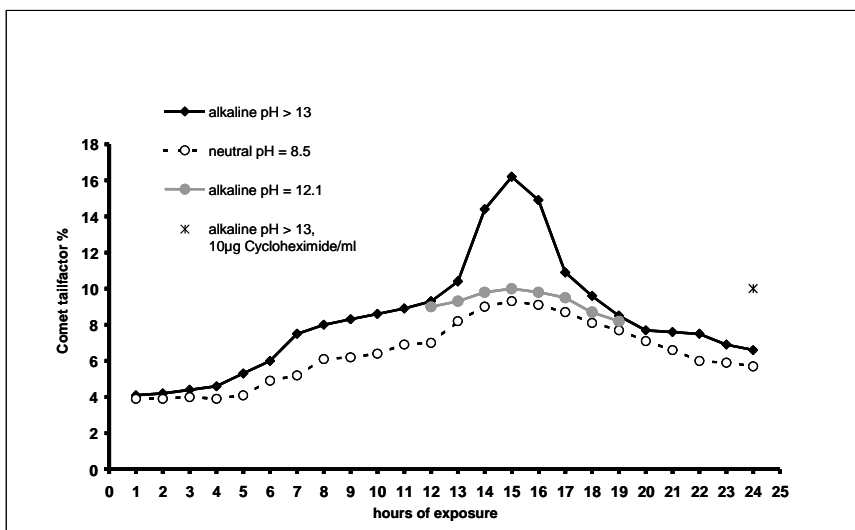


Figure 18. Comet assay of exposed human fibroblasts was performed at different pH (1 mT, intermittent 5 min on/10 min off)

DNA repair deficient cells react differently to ELF-EMF exposure.

Diploid human fibroblasts from patients with the genetically determined DNA repair defects Cockayne Syndrome, Ataxia Teleangiectatica, and Bloom Syndrome were obtained from Coriell Cell Repository (Camden, New Jersey, USA). The cells were cultured under standardized conditions and exposed (24 hours, 1 mT, 5 min on/10 min off) or sham exposed, and alkaline Comet assay was performed as described. As a result the Cockayne and Bloom Syndrome fibroblasts exhibited a similar pattern of genotoxicity as normal control fibroblasts, whereas the cells from a patient with Ataxia Teleangiectatica showed an almost threefold increased ELF-EMF induced Comet tailfactor as compare to normal cells (Figure 19).

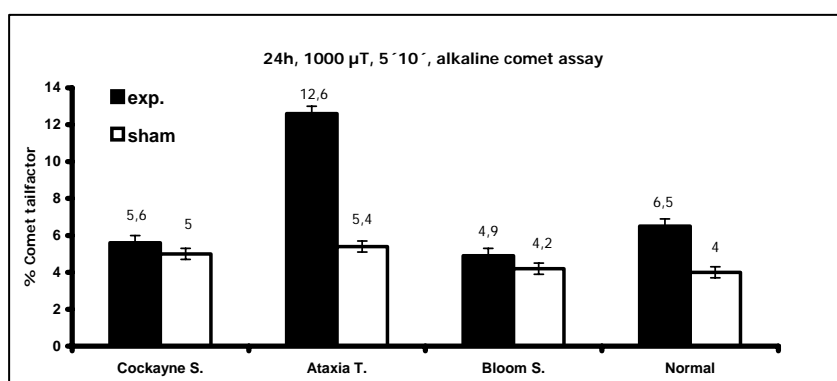


Figure 19. Alkaline Comet assay tailfactors of ELF-EMF exposed human fibroblasts from patients with various genetically determined DNA repair defects and normal controls.

Generation of DNA strand breaks through ELF/EMF was cell type specific.

ELF-EMF exposure (50 Hz sinusoidal, 1 mT, 5 min on/10 min off, 1-24 hours) of different human cell types (melanocytes, skeletal muscle cells, fibroblasts, monocytes, stimulated and quiescent lymphocytes) and of SV40 transformed rat granulosa cells revealed differences in induced DNA damage. Rat granulosa cells exhibited the highest DNA strand break levels and seemed to be most sensitive to intermittent ELF-

EMF exposure (Figures 20, 21). Human melanocytes also reacted, but not as strong as fibroblasts or rat granulosa cells. In contrast, stimulated or non-stimulated lymphocytes, monocytes and skeletal muscle cells did not respond at all.

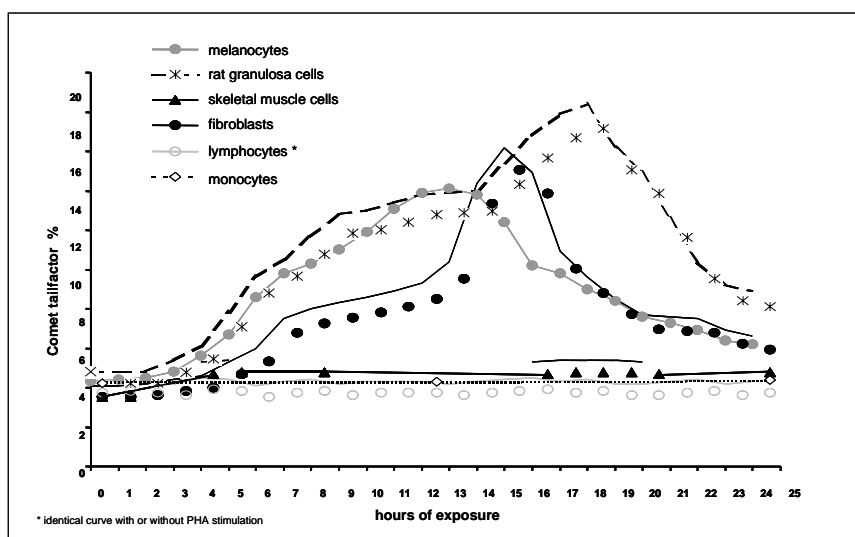


Figure 20. Alkaline Comet tailfactors of different human cell types (fibroblasts, melanocytes, monocytes, lymphocytes, skeletal muscle cells) and SV 40 transformed rat granulosa cells exposed to ELF-EMF (50 Hz sinusoidal, 1 mT, intermittent 5 min on/10 min off) for 1 to 24 hours.

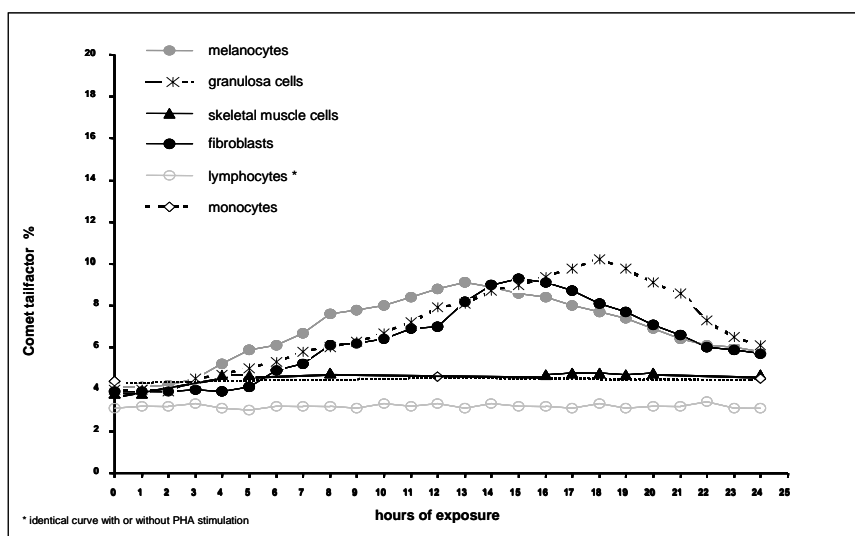


Figure 21. Neutral Comet tailfactors of different human cell types (fibroblasts, melanocytes, monocytes, lymphocytes, skeletal muscle cells) and SV 40 transformed rat granulosa cells exposed to ELF-EMF (50 Hz sinusoidal, 1 mT, intermittent 5 min on/10 min off) for 1 to 24 hours.

Generation of DNA strand breaks in human fibroblasts through ELF-EMF and their repair were modified by UVC or heat stress.

To test a possible impact of ELF-EMF exposure on DNA repair, cells were subjected to combined exposures to ELF + UVC or ELF-EMF + heat stress. In the first set of experiments fibroblasts were pre-exposed to UVC (10 min., 1.2 kJ/m²). Subsequently, ELF-EMF exposure (50 Hz, sinus, 1000 μT) was varied from 1-24 hours. Results of the alkaline Comet assay showed that DNA damage caused by UVC could be removed within 7 hours of ELF-EMF exposure (Figure 22). UV/ELF-EMF exposed cells

resulted in 50 % higher Comet assay levels than UV/sham exposed cells after 1 hour of ELF-EMF exposure. In UV/ELF-exposed cells DNA-damage was repaired very slowly, but the maximum at 15 hours ELF-EMF-exposure could not be detected any more. The results were similar with the neutral Comet assay, but DNA damage (DNA double strand breaks) was repaired within a shorter time (Figure 23)

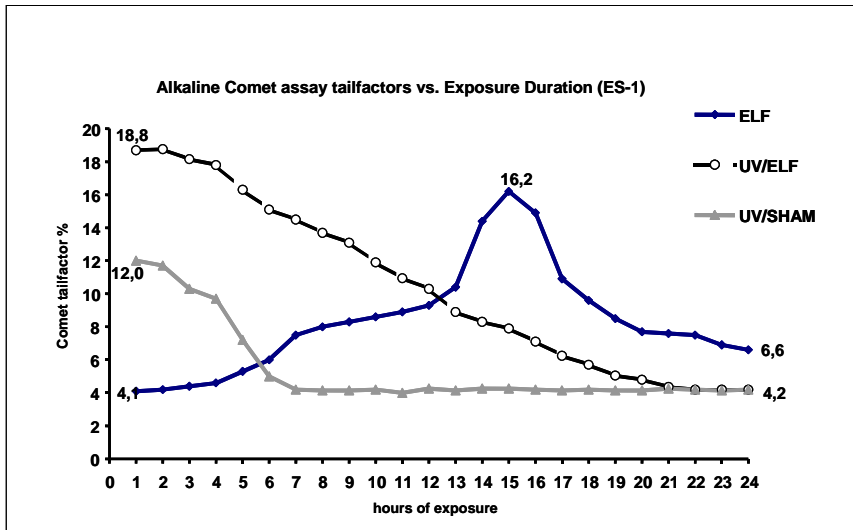


Figure 22. Repair kinetics of DNA single and double strand breaks in human fibroblasts (cell strain ES-1) after exposure with UV-C, ELF-EMF or UV C + ELF-EMF (cell strain ES-1, 1 mT, 5 min on/10 min off cycles) using alkaline Comet assay

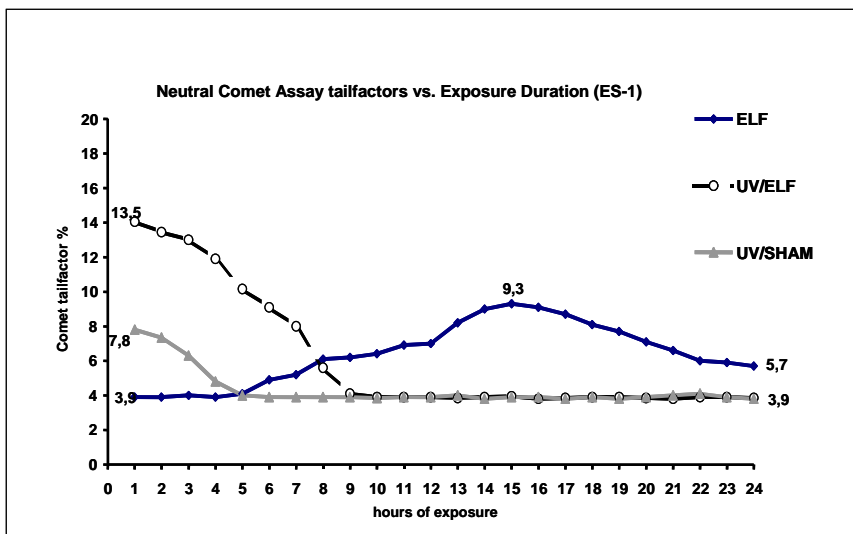


Figure 23. Repair kinetics of DNA single and double strand breaks in human fibroblasts (cell strain ES-1) after exposure with UV-C, ELF-EMF or UV C + ELF-EMF (cell strain ES-1, 1 mT, 5 min on/10 min off cycles) using neutral Comet assay

Based on the results with human fibroblasts, which suggest an induction of DNA repair upon intermittent ELF-EMF exposure, we concluded that pre-exposure to ELF-EMF would have a protective effect and diminish effects of additional exposures from other genotoxic factors. To check this assumption, fibroblasts were pre-exposed to ELF-EMF (50 Hz sinusoidal, 5 min on/10 min off, 1 mT) for 20 hours to ensure maximum induction of DNA repair. Subsequently, cells were either exposed to UVC (254 nm, 4.5

kJ/m^2 , 30 min) or to mild heat stress (38.5°C , 4 h). Recovery of DNA damage was evaluated using alkaline and neutral Comet assay. UVC-exposure produced 50 % higher DNA strand break levels than ELF-EMFs alone and DNA damage was completely repaired after 3 hours (Figure 24). DNA damage induced by mild thermal stress was even higher and persisted longer than 6 hours after exposure termination. Pre-exposure to ELF-EMF intensified and elongated UVC or temperature induced DNA damage. After 24 hours of recovery time ELF-EMF pre-exposed cells still exhibited higher DNA strand break levels and just about 50% of the initially induced DNA damage had been repaired after this time. The results were similar with the neutral Comet assay, indicating induction and repair of DNA double strand breaks (Figure 25).

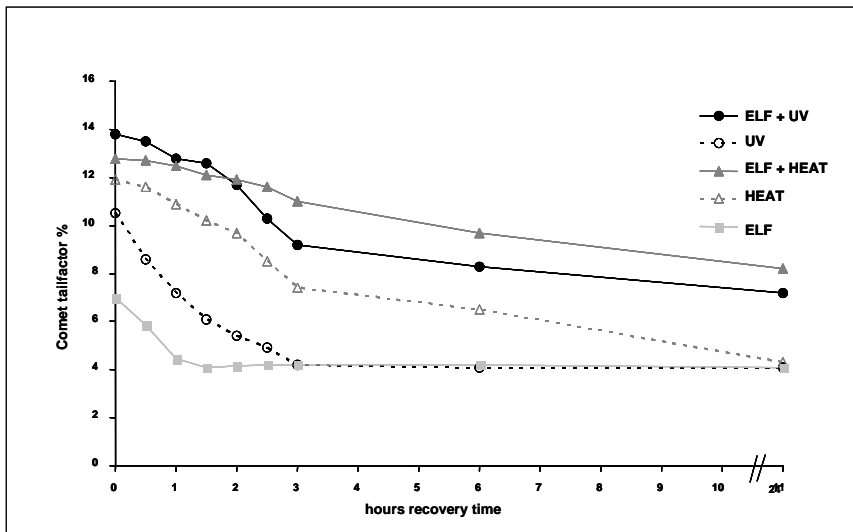


Figure 24. DNA damage and repair of cultured human fibroblasts pre-exposed to ELF-EMF (50 Hz sinusoidal, 5 min field-on/10 min field-off, 1 mT, 20 hours) and additionally exposed to UVC (254 nm, 30 min, 4.5 kJ/m^2) or mild thermal stress (38.5°C , 4 hours) evaluated using alkaline Comet assay.

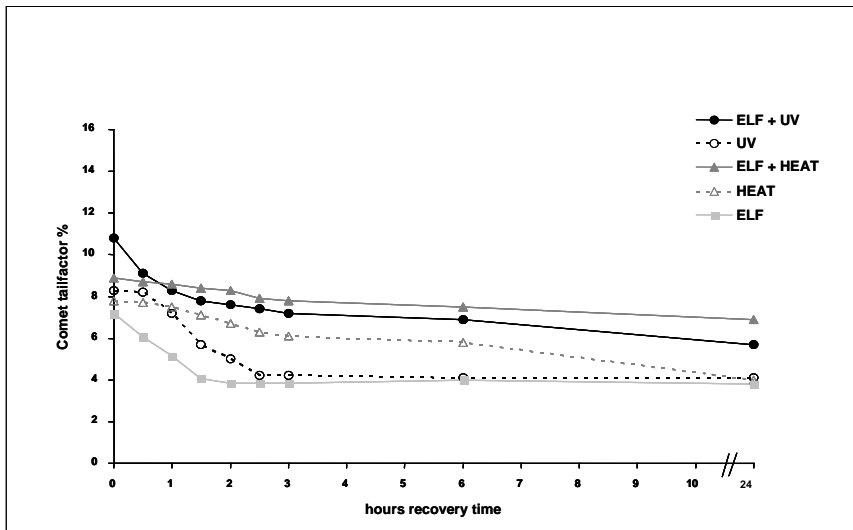


Figure 25. DNA damage and repair of cultured human fibroblasts pre-exposed to ELF-EMF (50 Hz sinusoidal, 5 min field-on/10 min field-off, 1 mT, 20 hours) and additionally exposed to UVC (254 nm, 30 min, 4.5 kJ/m^2) or mild thermal stress (38.5°C , 4 hours) evaluated using neutral Comet assay.

ELF-EMF generated chromosomal aberrations in human fibroblasts.

Chromosomal aberrations were evaluated at exposure conditions producing maximum effects in the Comet assay and in the micronucleus test (15 h, 1 mT, 5min on/10 min off). Five different types of aberrations were separately scored (gaps, breaks, rings, dicentric chromosomes, acentric fragments). Significant increases ($p < 0.05$) between exposed and sham exposed cells could be demonstrated for all types of aberrations (Table 6). Gaps were 4-fold increased, breaks 2-fold, and dicentric chromosomes and acentric fragments 10-fold. Translocations were evaluated using the fluorescence in situ hybridisation (FISH) technique. 1,000 metaphases were scored for each specifically labeled chromosome (1-22, X and Y) after ELF-EMF exposure (50 Hz, 24h, 5 min on/10 min off, 1 mT). No stable translocation in any of the 24,000 metaphases of ELF-EMF exposed cells could be detected (data not shown).

Table 6. Percentage of chromosomal aberrations induced by ELF-EMF exposure (50 Hz, 5' field-on/10' field-off, 1 mT, 15 h) in cultured human fibroblasts.

Types of aberrations	ELF-exposed (% \pm SD)	sham-exposed (% \pm SD)	p-value*
chromosome gaps	24.3 \pm 1 %	5.5 \pm 0.7 %	< 0.001
chromosome breaks	2.2 \pm 0.3 %	1.3 \pm 0.3 %	0.0015
ring chromosomes	0.1 \pm 0.07 %	---	0.0133
dicentric chromosomes	0.4 \pm 0.1 %	0.06 \pm 0.05 %	< 0.001
acentric chromosomes	0.3 \pm 0.07 %	0.02 \pm 0.04 %	< 0.001

^a A number of 1,000 metaphases were scored in each of five independent experiments. Results are expressed as percentage chromosomal aberrations per cell.

^b Significant differences ($p < 0.05$) as compared to sham-exposed controls using Student's t-test for independent samples

ELF-EMF did not alter the mitochondrial membrane potential in human fibroblasts.

The experimental settings in the present tests were based on conditions, which resulted in the highest inducible frequencies of these DNA strand breaks in human fibroblasts. Evaluating changes in the mitochondrial membrane potential after ELF exposure (50 Hz, 15 hours, 1 mT, 5 min on/10 min off) using JC-1, revealed no significant differences between exposed and sham-exposed fibroblasts.

3.1.1.2 Granulosa cells of rats, Chinese hamster ovary cells (CHO) and HeLa cells (Participant 7)

ELF-EMF exposure caused a significant increase of DNA strand breaks in cultured rat granulosa cells, CHO cells and HeLa cells.

The effect of ELF-EMF was analysed on the genomic level by use of the Comet assay. Especially the dependence on exposure time and frequency was analysed. Figure 26 shows that exposure to ELF-EMF at 16 2/3 Hz (5 min on/10 min off, 1.0 mT) caused a significant increase in single and double DNA strand breaks in cultured granulosa cells. The same result was obtained with CHO and HeLa cells (not shown). The data presented in Figure 26 indicate that the genotoxic effect at 16 2/3 Hz is time dependent with a maximum after about 18 hours of exposure, which resembles the results obtained at 50 Hz by Participant 3 (Ivancsits et al., 2003).

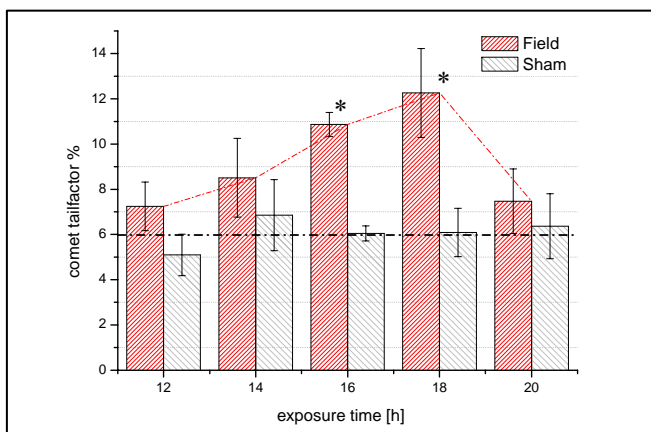


Figure 26. DNA damage of rat granulosa cells after exposure for 12 to 20 hours to ELF-EMF (16 2/3 Hz, 5 min on/10 min off, 1 mT) evaluated using alkaline Comet assay. For values of n see Material and Methods. (* $p < 0.05$)

To investigate the frequency dependence of the genotoxic effect of ELF-EMF (5 min on/10 min off) exposure of rat granulosa cells a constant exposure time of 18h was selected. Figures 27 and 28 present the tailfactors of exposed and sham exposed granulosa cells using the alkaline and neutral Comet assay. At the applied frequencies within the range of 8 Hz to 1000 Hz a significant frequency dependence was not observed for the rate of double DNA strand breaks as derived from the neutral Comet assay (Figure 28). The corresponding results of the alkaline Comet assay are presented in Figure 27. At 8 Hz, 16 2/3 Hz and 50 Hz an intensity of 1 mT could be applied (Figure 27a). A significant increase of DNA strand breaks was found at 16 2/3 Hz. Surprisingly, especially at 50 Hz the s.e.m. data of sham and ELF-EMF exposed cells differ significantly. The large error could be caused by a variable time dependent location of the maximum and/or the influence of the specific cell passage. Further experiments are under analysis to confirm the data presented in Figure 27a. At 1000 Hz the recorded DNA damage is significantly lower than observed at 16 2/3 Hz (Figure 27b). But it has to be noted that the maximal applied flux density was limited to 0.6 mT due to the used exposure system (Participant 10). Furthermore, DNA damage was measured at 20 μ T, which approximately corresponds to the maximal acceptable magnetic flux density as recommended by the 26. BImSchV¹. Again a significant increase of DNA strand breaks was observed (Figure 27b).

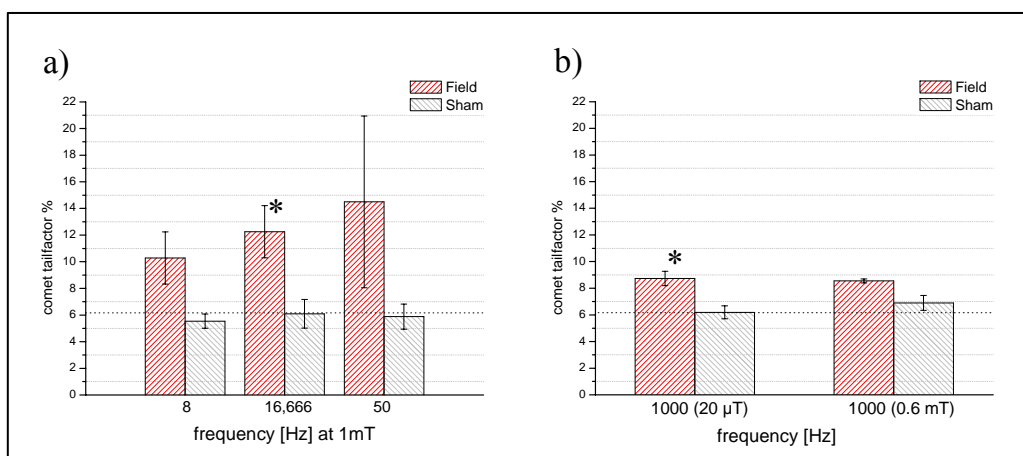


Figure 27. DNA damage of rat granulosa cells as function of frequency of ELF-EMF (5 min on/10 min off) after exposure for 18 hours as derived by the alkaline Comet assay. **a)** In the frequency range of 8 to 50 Hz the flux density was set to 1 mT. **b)** At 1000 Hz the flux density was adjusted to 20 μ T and 0.6 mT (for further explanation, see text). For values of n see Material and Methods. (* $p < 0.05$)

¹ 26. Verordnung zur Durchführung des Bundes-Immissionschutzgesetzes (Verordnung über elektromagnetische Felder – 26. BImSchV)

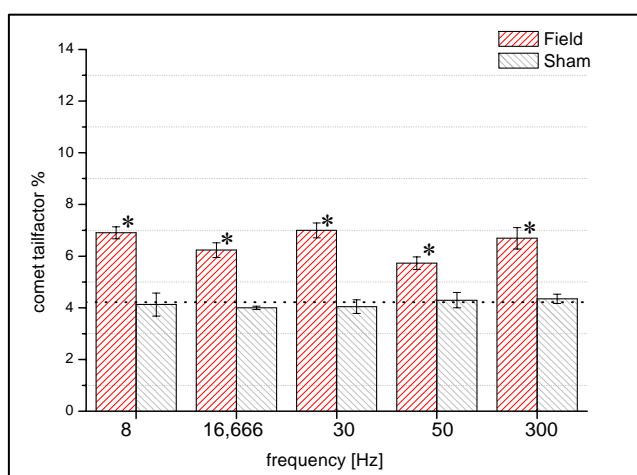


Figure 28. Double DNA strand breaks of rat granulosa cells as function of frequency of ELF-EMF (5 min on/10 min, 1 mT) after an exposure time of 18 hours as derived by the neutral Comet assay. For values of n see Material and Methods. (* p< 0.05)

3.1.1.3 Embryonic stem cells (ES) of mice (Participant 4)

Lack of effects on single and double strand break induction 0, 18, 24 and 48 hours after completion of a 6 or 48 hours ELF-EMF exposure.

The effects of ELF-EMF on the integrity of DNA strands in differentiating ES cell from EB outgrowths were studied. Two schemes were applied: (1) For ELF-EMF exposure (50 Hz Powerline, 2.0 mT, 5 min on/30 min off, 6 hours) the percentage of primary DNA damage was measured immediately after ELF-EMF exposure at the stage of neural differentiation (4+4d - 4+6d) and 18 hours after exposure using the alkaline and neutral Comet assay. (2). In the second set of experiments, the same ELF-EMF exposure conditions were applied for 48 hours instead of 6 hours, and the alkaline Comet assay was done immediately after exposure, while the neutral Comet assay was done 24 or 48 hours post exposure. No significant differences were observed in the induction of single or double DNA strand breaks between sham-exposed or ELF-EMF exposed neural progenitors.

3.1.1.4 Summary (Participant 1)

Our data indicate a genotoxic action of ELF-EMF in various cell systems. This conclusion is based on the following findings:

- Intermittent exposure to 50 Hz ELF-EMFs generated DNA single and double strand breaks in various cell systems such as human fibroblasts, melanocytes, granulosa cells of rats, Chinese hamster ovary cells (CHO) and HeLa cells, but not in human lymphocytes, monocytes, myelocytes and neural progenitors from mouse embryonic stem cells (see 3.1.1.1, 3.1.1.2 and 3.1.1.3).
- DNA damage generated by ELF-EMF in human fibroblasts was dependent on time and dose of exposure, on the age of the donors the cells derived from, and on the genetic background of the cells. A flux density of 35 μ T was high enough to significantly increase the number of DNA strand breaks (see 3.1.1.1)
- The increase in DNA strand breaks in human fibroblasts due to ELF-EMF exposure was accompanied by an enhanced formation of micronuclei which was also dependent on the exposure time (see 3.1.1.1).
- The DNA repair system in human fibroblasts which was strongly activated by ELF-EMF during exposure did not work error-free as shown by a significant increase of different types of chromosomal aberrations (see 3.1.1.1).
- Genotoxic effects were frequency dependent. Significant increases in DNA strand breaks were found, when an ELF-EMF of 3 Hz, 16 2/3 Hz, 30 Hz, 50 Hz, 300 Hz, 550 Hz and 1000 Hz was applied. The

effect was strongest with 50 Hz ELF-EMF and second strongest with 16 2/3 Hz (see 3.1.1.1 and 3.1.1.2).

3.1.2 Cell proliferation and differentiation

3.1.2.1 Human neuroblastoma cell line NB69 (Participant 5)

ELF-EMF promoted the growth rate of NB69 neuroblastoma cells.

Immunocytochemical staining using antibodies against phenotype-specific antigens revealed that NB69 cells contain the neuroblast-specific protein β III-tubulin. However, these cells do not contain the neuroepithelial marker nestin, which is present in immature progenitors and in some neuroblastoma cells, nor the astrocyte-specific antigen GFAP. The cells remained in an undifferentiated state throughout the experimental period. Only the treatment with retinoic acid induced neurite extension accompanied by cell growth reduction.

Two series of experiments were carried out to analyse the cell growth response of NB69 cells to ELF-EMF. In the first series, the ELF-EMF administered alone (42 hours) provoked a modest, though significant increase in the number of cells at day 5 postplating (5 dpp), both at 10- μ T (12% over controls, $**p < 0.01$) and 100- μ T MFD (17 % increase over controls, $***p < 0.001$) as shown in Figure 29A). Retinol (ROL) alone or in combination with ELF-EMF did not change significantly the cell growth (data not shown). The ELF-EMF exposure also provoked modest increases in the total DNA levels, the effect being statistically significant at 10 μ T (8 % over controls, $p < 0.05$, Figure 29B). However no significant changes were observed in the protein or protein/DNA contents in the ELF-EMF exposed samples. Taken as a whole, these results indicate that exposure to 50 Hz ELF-EMF at 10 or 100 μ T promote cell growth in the NB69 human neuroblastoma cell line.

In the second series of experiments, the 42-hours exposure to ELF-EMF at a flux density of 100 μ T significantly increased cell growth (11 % over controls, $***p < 0.001$, Figure 30A). This result confirms the growth-promoting response obtained in the first experimental series. However, such an effect was not observed, when the ELF-EMF exposure was maintained for a longer period of time, i.e. 90 hours (Figure 30B). The treatment with retinoic acid (RA) alone significantly reduced the cell number, both at 42 and 90 hours, when compared to untreated controls. Also, RA-treated cells did show the growth-promoting effects of a 100 μ T ELF-EMF, these samples demonstrating reduced growth rates when compared to unexposed controls: 35% reduction at the end of 42 hours-treatment ($p < 0.0001$) and 57% reduction at the end of 90 hours-treatment ($p < 0.0001$).

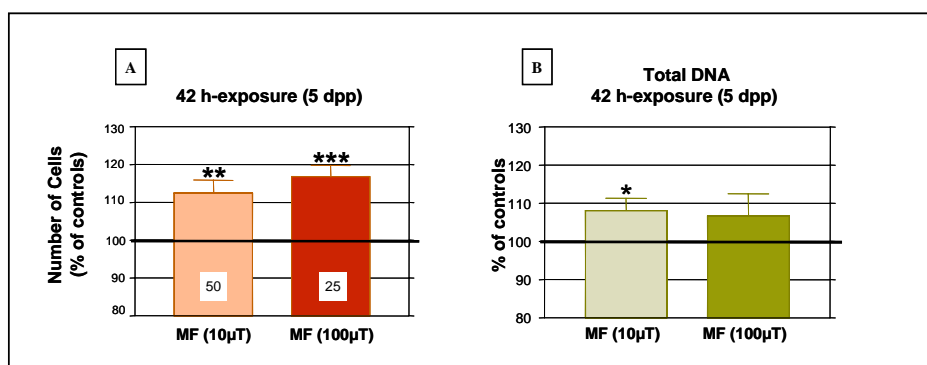


Figure 29. First series of experiments. A-Cell growth estimated by cell counting (Trypan blue exclusion) and B-Total DNA estimated by spectrophotometry.

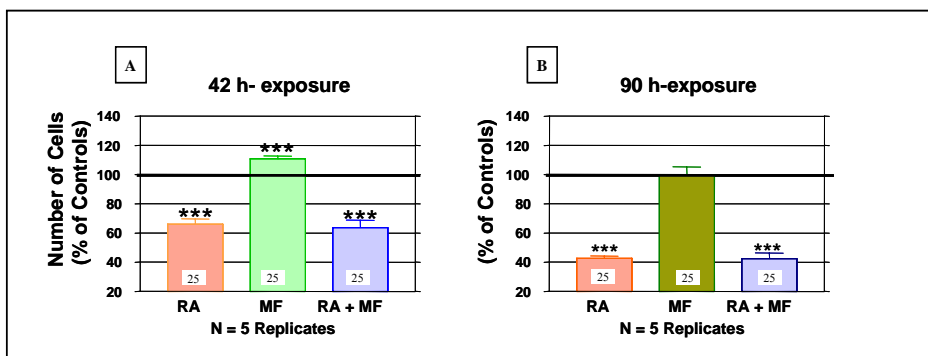


Figure 30. Second series of experiments: A-Number of cells at day 5 postplating (after 42 hours-exposure) and B-Number of cells at day 7 postplating (after 90 hours-exposure).

No experiment could be performed at a flux density of 2.0 mT following the 3 hours on/3 hours off exposure protocol, since the ohmic heat in the coils due to the electric current could not be compensated by the incubator resulting in an unstable ambient temperature. When the samples were exposed to 2 mT ELF-EMF in a 5min on/30 min off cycle, no effect was observed on the cell growth. Similarly, the cells did not respond to a 5 min on/30 min off cyclic exposure to a 100 μ T ELF-EMF. It is possible that the NB69 cell line requires a longer exposure cycle to show significant changes in the cell growth.

A growth-promoting effect of ELF-EMF in NB69 neuroblastoma cells was not observed after an extended exposure period.

As described above, the growth promoting effect of a 100- μ T EMF was not observed when the exposure was maintained for a longer period of time, i.e. 90 hours (Figure 30B). In NB69 cultures kept in control conditions, the number of cells peaks at day 6 and then decays (Figure 31). In the present experiments, long-term cultures (7 days postplating) reached a confluence stage close to saturation. This physiological condition could be the cause of the lack of response to ELF-EMF after long-term exposures between 3 and 7 days postplating.

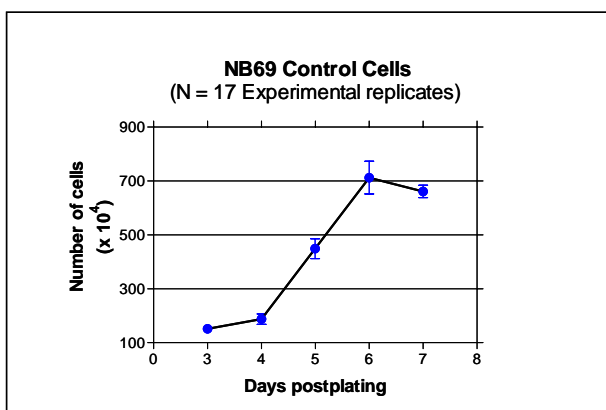


Figure 31. Growth pattern of NB69 cells: On day 7 the number of cells is reduced when compared to that at day 6. Long-term cultures (7 days postplating), reached a confluence stage close to saturation.

ELF-EMF did not counteract the retinoic acid-induced inhibition of cell proliferation in NB69 neuroblastoma cells.

To better characterise the potential ELF-EMF effects on the proliferation/differentiation rate, NB69 cells were treated with a chemical agent that inhibits proliferation and induces differentiation. All trans retinoic

acid (RA) promotes differentiation in NB69 cells, inducing outgrowth of long neurite-like processes and driving of the cell morphology along a neural pathway. As shown in Figure 30AB, the cell growth decreases after treatment with RA (2 μ M) for 5 or 7 days. This response to RA remained unchanged after exposure to the ELF-EMF during 42 or 90 hours.

ELF-MF enhanced the cellular proliferation rate NB69 neuroblastoma cells as revealed through analysis of cell proliferation markers (PCNA).

Studies of expression of cell proliferation markers (PCNA) reinforce the described effects of ELF-EMF on cell growth: To determine whether the above growth-promoting effect detected by Trypan Blue exclusion involves changes in cell proliferation, we searched for changes in the proliferating cell nuclear antigen (PCNA). PCNA immunolabelling shows that exposure to 10 μ T ELF-EMF significantly increases the proportion of PCNA-positive cells (24% increase; Figure 32). This effect was associated with an increase in the number of cells (15% increase), showing a significant linear correlation between both of the parameters, PCNA positive cells and total number of cells, at the end of 42 hours exposure ($p < 0.01$). These results confirm and reinforce the previous observations that a 42 hours exposure to ELF-EMF at a flux density of 10 μ T can modulate cell growth in NB69 cells. The mean value of PCNA positive cells in controls is 32 % \pm 1,3).

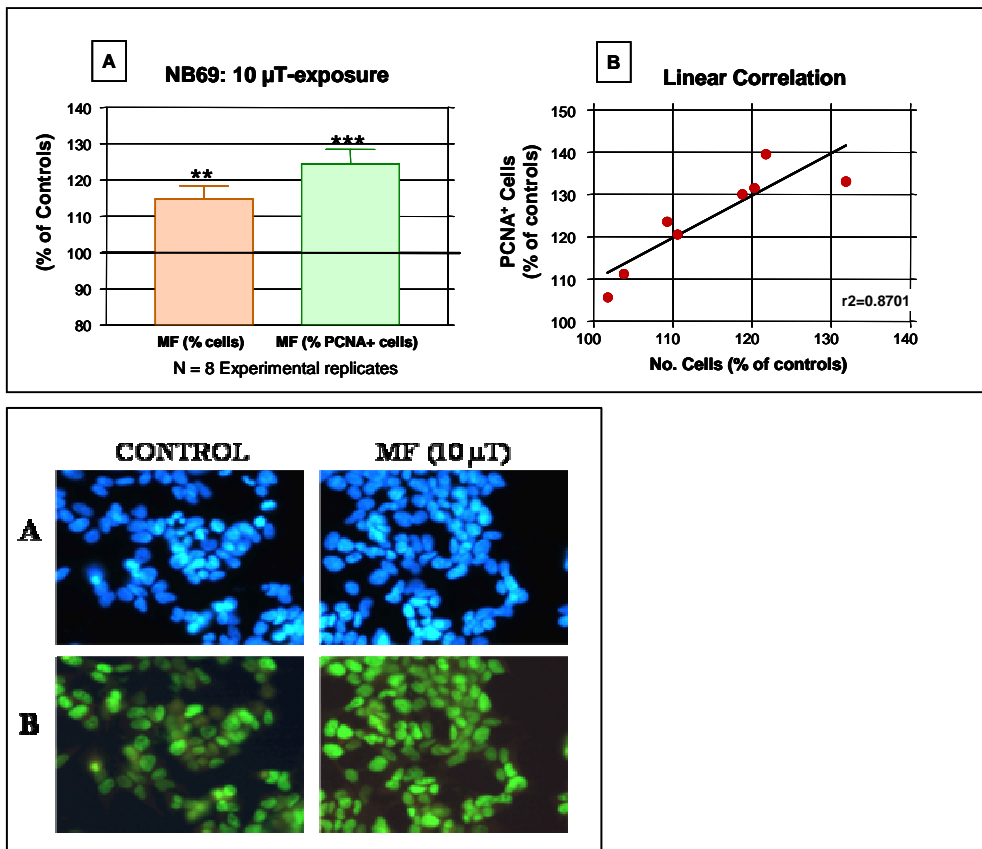


Figure 32. A) Growth response of NB69 to 10 μ T after a 42 hours exposure as revealed by Trypan (brown) and PCNA content (green). Student T' test: ** $p < 0.01$; *** $p < 0.001$. B) Linear correlation between these two parameters. Photomicrographs of NB69 cells. A: Hoechst-marked nuclei. B: PCNA labelling. The ELF-EMF exposure induced an increase in the number of cells expressing PCNA.

Neuroblastoma cell cultures contain two different phenotypes. One type is characterised by flattened, "sail-like" morphology and shows a strong adherence to the culture flask. These cells are called S-cells. The second phenotype corresponds to much smaller, triangular cells that adhere to the culture flask loosely. These cells, called N cells have a neuroblastic phenotype, are clonogenic and tumorigenic and

grow rapidly in the culture flask. We have observed that the relative proportion of both phenotypes evolves along the successive subcultures, which seems to significantly influence the response of the culture, as a whole, to the field exposure. In fact, young passages, having a high proportion of N cells, are particularly sensitive to ELF-EMF, whereas older passages, very rich in S-cells and with virtually no N cells, are not responsive to ELF-EMF exposure. Consequently, we conducted experiments with young passages, where the cells were exposed to a 100- μ T ELF-EMF during 63 hours (day 6 post-plating). A significant increase in the number of cells was observed in the exposed samples (9.7% over controls $p < 0.0001$, Figure 33A). The mean cell number in controls was $621.689 \pm 62.314 (x10^4)$. The increase in the number of cells was found to be associated with significant increases in the proportion of PCNA-positive cells. Figure 33B shows the percent of PCNA positive cells at days 5 and 6 post-plating (dpp). Only at 6 dpp significant changes in the number of PCNA positive cells were observed (31.7% over controls, $p < 0.01$, $N = 3$ experimental replicates). Those changes do not represent an ELF-EMF-induced increase in PCNA labelling, since the percent of PCNA positive cells in the control cultures spontaneously decreased between days 5 and 6 post-plating (Student T'test *, $p < 0.05$). Such a decrease did not occur in the exposed cultures. The present results indicate that the regulation of the kinetics of the cell cycle could be altered by ELF-EMF at 100 μ T. Provided that in the proliferating cell the PCNA levels are maximal at late G1 and S phases, it is possible that such phases of the cell cycle are implicated in the above described responses.

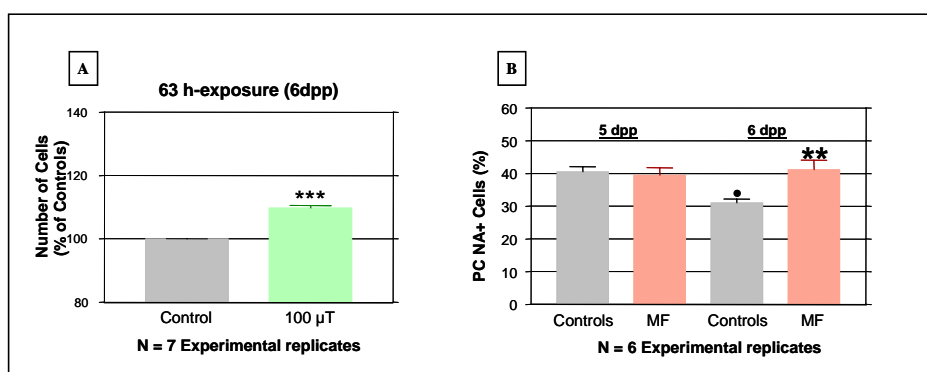


Figure 33. A) Percent of cells at the end of 63-hours exposure and/or incubation (6 day post-plating). B) Percent of PCNA positive cells at 5-6 days post-plating (dpp). In controls the percent of PCNA positive cells significantly decreases between the days 5 and 6 post-plating (Student T'test •, $p < 0.05$), whereas in exposed cells at 100 μ T this decrease did not occur).

ELF-EMF increased the DNA synthesis in NB69 neuroblastoma cells.

We also tested the BrdU incorporation into DNA. As shown in Figure 31, at the end of a 42-hours exposure (5 pp) to the 100 μ T ELF-EMF a significant increase of BrdU- positive cells was observed in the treated cultures (41 % over controls, Student's T test $p < 0.01$). Such an effect was followed (63-hours exposure, 6 pp) by a subsequent increase in the number of cells (9.7% over controls, $p < 0.001$, Figure 34). This response was accompanied by a significant reduction in the percent of spontaneously apoptotic cells (58.5 % of that in controls, $p < 0.05$).

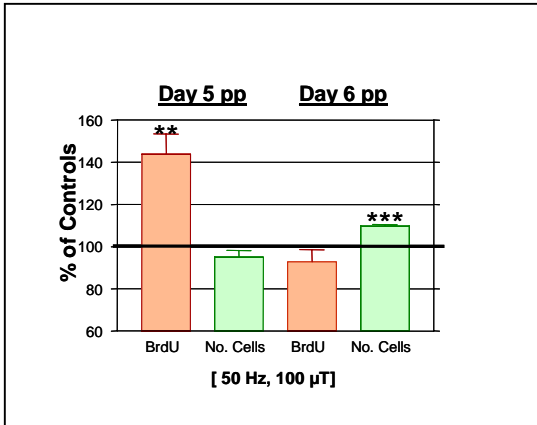


Figure 34. Cell growth in a total of 18 experiments: ELF-EMF effects at 5 days post-plating (42 hours exposure) or at 6 days post-plating (63 hours exposure): Red, percent of BrdU-positive cells; Green, Number of Cells analysed by Trypan blue exclusion. Student T'test: ** $p < 0.01$; *** $p < 0.001$.

ELF-EMF affected the cell cycle in NB69 neuroblastoma cells.

The experiments performed to test the DNA content and the cell cycle distribution by flow cytometry showed that at the end of day 5 post-plating (Figure 35A), the 42-hours exposure to 100 μ T ELF-EMF induces increases in the number of cells in G2-M phase of the cell cycle (28% over controls; N= 3 experimental replicates). The exposure also provoked a modest reduction of cells in G0-G1. However, no significant changes were observed in the number of cells in S-phase and in the number of total cells (Trypan Blue exclusion, Figure 352A). The flow-cytometry assay at the end of day 6 post-plating did not reveal EMF-induced changes in the cell cycle (G0-G1; S and G2-M), even though a significant increase in the number of alive cells was observed (16.7% over controls, $p < 0.05$; N= 5 experimental replicates, Figure 35B). These results confirm and reinforce our previous observations using other techniques, that 100 μ T 50-Hz ELF-EMF can promote cell growth in the NB69 cell line from a human neuroblastoma.

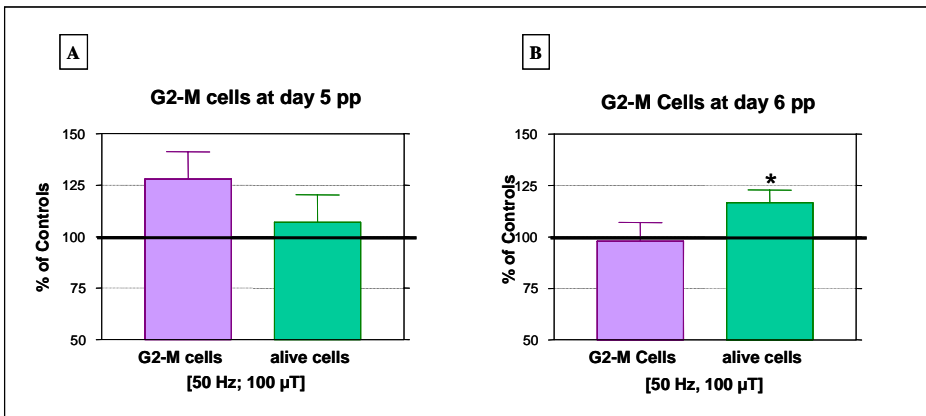


Figure 35. A) A 42 hours-exposure to a 100- μ T field provokes an increase in the percent of G2-M cells at day five postplating (5 pp). B) This increase was not observed one day later, after 63 hours- exposure, however, a significant increase in the number of alive cells occurred.

ELF-EMF diminished the spontaneous apoptosis in NB69 neuroblastoma cells.

In order to investigate the potential influence of 50 Hz ELF-EMF on apoptosis the percent of apoptotic cells was estimated with TUNEL-labelling after 63 hours of exposure. Also, the number of cells was

quantified by Trypan Blue exclusion. The results (Figure 36A) indicate that ELF-EMF of 50 Hz at a flux density of 100 μ T (3 hours on/3 hours off) induces a significant reduction in the spontaneous apoptosis of the NB69 cell line. This response was associated with an increase in the number of cells (9.7% over controls, $p < 0.001$, Figure 36B as we previously observed in experiments described above. Apoptosis was also determined through flow cytometry analysis; the results confirming a reduction at the end of 63 hours-exposure (data not shown).

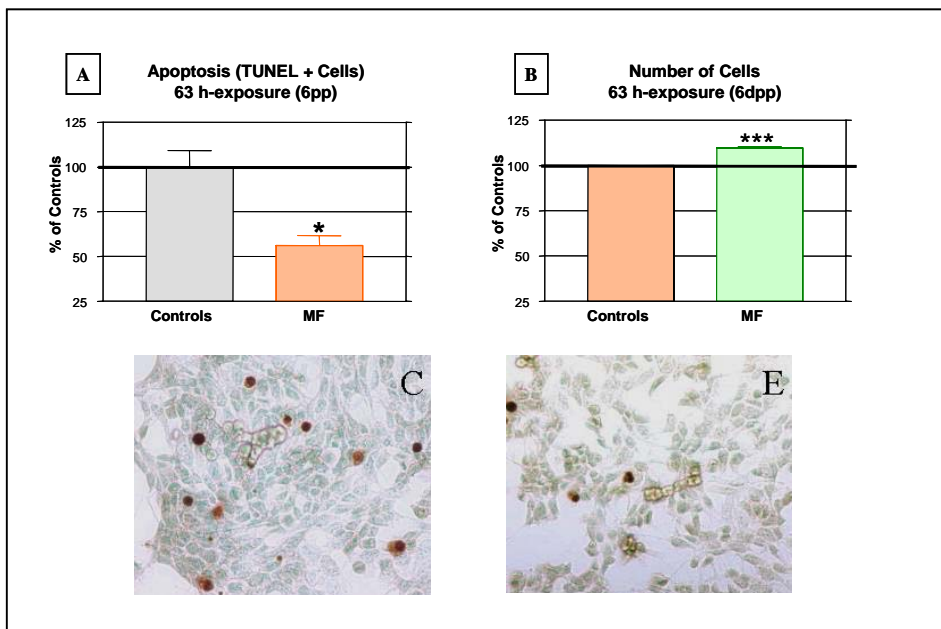


Figure 36. A) ELF-EMF (50 Hz, 100 μ T) induce a significant reduction in the spontaneous apoptosis of the NB69 cell line. B) This described response is associated with an increase in the number of cells. (* $p < 0.05$, *** $p < 0.001$, Student T' test, three independent experimental replicates). Photomicrographs showing TUNEL-positive cells in controls (C) and exposed (E) samples.

ELF-EMF altered the activation of the phosphorylated cyclic adenosine monophosphate response-element binding protein (p-CREB).

The results of a total of 8 experiments show that both, the labelling/cell in NB69 cells and the proportion of phospho-CREB positive cells increase after 60 min of exposure (35.4% over controls, $p < 0.01$, Figure 37 and photomicrograph). The percent of p-CREB positive cells in controls after 60 min of exposure was 32%. However, no differences were observed between ELF-EMF-exposed and controls samples after 30 or 120 min of exposure. These preliminary results suggest that the activation of p-CREB is involved in the previously described effects of 50 Hz 100 μ T ELF-EMF on cell growth/apoptosis. In additional experiments the analysis of Western confirms that the ELF-MF induced a short-time dependent activation of the transcriptional factor CREB, with a peak at 60 min followed by a recovering of the basal levels at 120 minutes of exposure (data not shown).

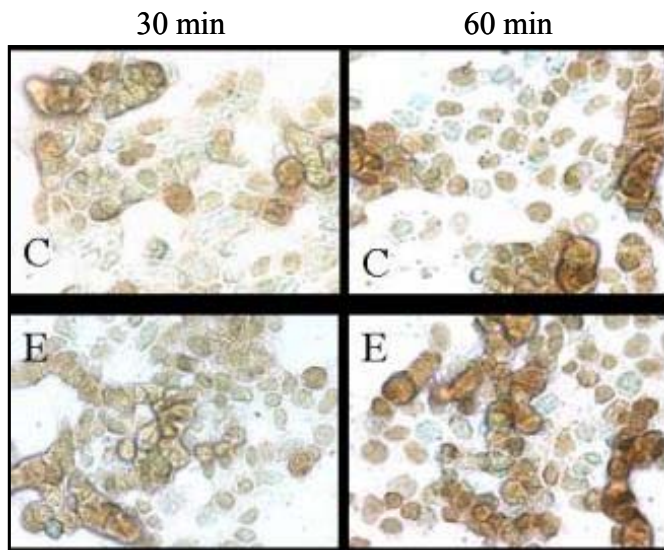


Figure 37. Immunocytochemistry for phospho-CREB. Changes in p-CREB positive cells showed a time-dependent response in the presence of the 100 μ T ELF-EMF. Photomicrograph showing the p-CREB labelling in brown and the counterstaining in green(methylgreen).

3.1.2.2 Embryonic stem cells of mice during cardiac differentiation (Participant 8)

ELF-EMF accelerated the cardiac differentiation of embryonic stem cells through enhanced expression of cardiac genes.

See 3.1.4.3

3.1.2.3 Human lymphocytes (Participant 8)

ELF-EMF exposure did not have any influence on proliferation, cell cycle and functionality of human lymphocytes.

The experiments with ELF-EMF (50 Hz) were performed at 50 μ T magnetic field intensity on cells from 20 donors. Cell proliferation, cell cycle together with membrane activation markers were studied on lymphocytes from young donors. Data obtained by all the experiments performed indicated that no significant differences exist on cell proliferation or DNA synthesis at any time during the continuous exposure up to 6 days, as well as on cell cycle during the continuous exposure up to 96 hours. Cell activation phase was studied on CD3+HLA-DR+ T lymphocytes and CD4+CD25+ T helper lymphocyte subpopulation, but also in this case no differences were found between cells exposed and not exposed.

3.1.2.4 Embryonic stem cells of mice (Participant 4)

ELF-EMF did not have any influence on the growth and neuronal differentiation of embryonic stem cells of mice.

See 3.1.4.1

3.1.2.5 Summary (Participant 1)

Our data show some influence of ELF-EMF on proliferation and differentiation of some, but not all cell systems investigated. This conclusion is based on the following findings:

- ELF-EMF at a flux density of 0.1 mT significantly increased the proliferation of neuroblastoma cells (NB69 cell line) after exposure for 42- and 63-hrs (see 3.1.2.1).
- ELF-EMF at a flux density of 0.8 mT accelerated the cardiac differentiation of embryonic stem cells through enhanced expression of cardiac genes (see 3.1.2.2 and 3.1.4.3)

- ELF-EMF at a flux density of 2 mT did not have any influence on the growth and neuronal differentiation of embryonic stem cells of mice (see 3.1.2.4 and 3.1.4.1)
- ELF-EMF at a flux density of 0.8 mT did not have any influence on proliferation, cell cycle and activation of lymphocytes, either (see 3.1.2.3).

3.1.3 Apoptosis

3.1.3.1 Embryonic stem cells of mice (Participant 4)

ELF-EMF at a flux density of 2 mT up-regulated the transcript levels of the anti-apoptotic gene bcl2 and the growth arrest and DNA damage inducible gene GADD45 and down-regulated bax in ES cell-derived neural progenitor cells. This may indirectly influence the apoptotic process in neural progenitor cells.

See 3.1.4.1

3.1.3.2 Neuroblastoma cell line NB69 (Participant 5)

ELF-EMF at a flux density of 100 μ T inhibited the spontaneous apoptosis in NB69 neuroblastoma cells.

See 3.1.2.1

3.1.3.3 Human fibroblasts (Participant 3)

No differences in cell count between ELF-EMF exposed and sham exposed human fibroblasts at any exposure duration could be detected. Therefore a possible elimination of cells by apoptosis and cell death can probably be ruled out.

See 3.1.1.1

3.1.3.4 Summary (Participant 1)

Our data indicate that ELF-EMF may have some indirect effect on apoptosis in certain, but not all cell systems investigated. This conclusion is based on the following findings:

- ELF-EMF at a flux density of 2 mT up-regulated in neural progenitor cells the transcript levels of the GADD45 gene and down-regulated the transcript levels of the bax gene by which the apoptotic process may be modulated (see 3.1.3.1 and 3.1.4.1).
- ELF-EMF at a flux density of 0.1 mT inhibited the spontaneous apoptosis in neuroblastoma cells in a way which is at present not well understood (see 3.1.3.2 and 3.1.2.1).
- ELF-EMF at a flux density of 1 mT did neither measurably affect the apoptotic process nor could a cytotoxic effect be detected in human fibroblasts in the course of a 24h exposure (see 3.1.1.1 and 3.1.3.3).

3.1.4 Gene and protein expression

3.1.4.1 Embryonic stem cells of mice (Participant 4)

ELF-MF exposure resulted in up-regulation of egr-1, c-jun and p21 transcript levels in p53-deficient, but not in wild type ES cells.

To analyse the effects of ELF-EMF, undifferentiated wild type (wt) and p53-deficient ES cells were exposed at different intermittence schemes and flux densities of 0.1, 1,0 and 2.3 mT for 6 and 48 hours, respectively (Table. 7). The exposition of ES cells to 5 min on followed by 30 min off cycles applied at

the high flux density of 2.3 mT resulted in a statistically significant up-regulation of *egr-1*, *p21* and *c-jun* mRNA levels in p53-deficient ES cells (Figure 38A and C), whereas wild type cells showed no variations in transcript levels compared to sham exposure and control cells (Figure 38A). In contrast, low flux densities of 0.1 and 1 mT ELF-EMF applied at 5 min on/30 min off intermittence cycles induced no significant effects on transcript levels indicating that a high flux density of ELF-EMF signals is necessary to affect mRNA levels of regulatory genes (Table 7).

Table 7. Conditions of the exposure of p53-proficient and deficient pluripotent embryonic stem cells embryonic stem cells to ELF-EMF and summary of the effects on transcript levels of regulatory genes.

Intermittent exposure (5min on/30 min off)			
6 hours ELF-EMF exposure ; wt, p53 ^{-/-}		48 hours ELF-EMF exposure; wt, p53 ^{-/-}	
0.1 mT	no ELF-EMF effect (n=3)	0.1 mT	no ELF-EMF effect (n=3)
1.0 mT	no ELF-EMF effect (n=3)	1.0 mT	no ELF-EMF effect (n=3)
2.3 mT	up-regulation of <i>egr-1</i> , <i>p21</i> and <i>c-jun</i> in p53 ^{-/-} cells (without recovery time, RT); no ELF-EMF effect after 18 h RT (n=6)	2.3 mT	no ELF-EMF effect (n=3)

Intermittent exposure (5min on/10 min off)			
6 hours ELF-EMF exposure; wt, p53 ^{-/-} ; without RT		6 hours ELF-EMF exposure; wt, p53 ^{-/-} ; 18h RT	
2.3 mT	no ELF-EMF effect (n=6)	2.3 mT	no ELF-EMF effect (n=6)

Continuous exposure			
6 hours ELF-EMF exposure; wt, p53 ^{-/-}		48 hours ELF-EMF exposure; wt, p53 ^{-/-}	
0.1 mT	no ELF-EMF effect (n=3)	0.1 mT	no ELF-EMF effect (n=3)
1.0 mT	no ELF-EMF effect (n=3)	1.0 mT	no ELF-EMF effect (n=3)

ELF-MF exposure of p53-deficient cells induced only short-term and transient effects on gene expression levels.

To elucidate, whether ELF-EMF induce short- or long-term responses, p53-deficient and wt ES cells were exposed to intermittent 5 min on/30 min off ELF-EMF signals for 6 hours. In parallel, the cells were analysed after a recovery time of 18 hours. No statistically significant effects could be seen after 18 hours recovery in control, sham- and field-exposed variants suggesting that ELF-EMF induced only an immediate transient response in p53-deficient cells (Figure 38B). These observations correlated with the results of the 48 hours ELF-EMF exposure to p53-deficient ES cells at early differentiation stage, where no ELF-EMF effects on transcript levels were found (data not shown, see Table 7).

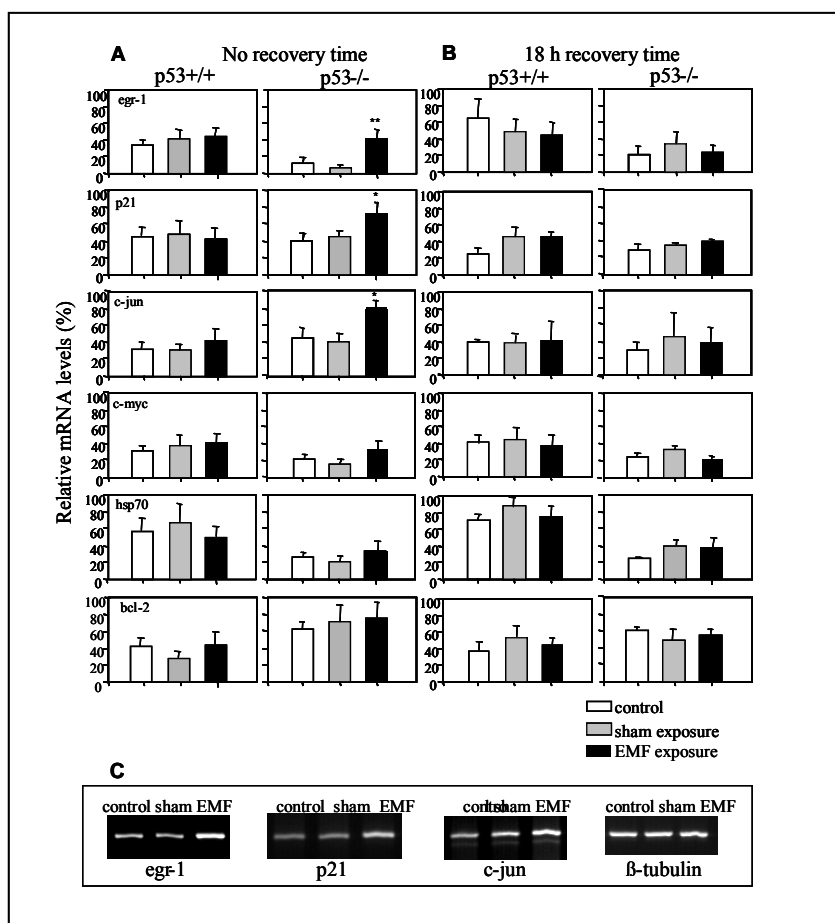


Figure 38. Relative mRNA levels of genes encoding egr-1, p21, c-jun, c-myc, hsp70 and bcl-2 in p53-deficient (p53^{-/-}) EC cell-derived embryoid bodies (EB) compared to wild-type (wt, p53^{+/+}) D3 cells immediately after 6h ELF-EMF (2.3 mT, intermittency 5 min on / 30 min off cycles) exposure (A) and after 18h recovery time (B) analysed by semi-quantitative RT-PCR. ELF-EMF exposure resulted in a significant, but transient up-regulation of egr-1, c-jun and p21 mRNA levels in undifferentiated p53-deficient (C), but not wt ES cells. Statistical significance was tested by Student's t-test for significance levels of 1% and 5% (**p<0.01; *p<0.05)

ELF-MF effects on transcript levels of regulatory genes in p53-deficient cells were dependent on intermittence cycles (on/ off cycle duration).

In addition, we analysed in wt and p53-deficient ES cells the influence of ELF-EMF signals applied at another intermittence scheme of 5 min on/10 min off for 6 hours with a flux density of 2.3 mT. We found that 5 min on/10 min off ELF-EMF signals with or without recovery time had no effects on the transcript levels of the investigated regulatory genes in both, wt and p53-deficient cells. Further, continuous ELF-EMF signals at flux densities of 0.1 and 1 mT were applied to wt and p53-deficient ES cells. We found no influence of continuous ELF-EMF on the mRNA levels of the regulatory genes included in the study (data not shown). Experiments with the highest flux density (2.3 mT) could not be performed with the continuous exposure protocol, because the generated ohmic heat of the coils could not be compensated by the incubator and would have resulted in an unstable ambient temperature.

ELF-EMF exposure up-regulated the transcript levels of bcl-2, the growth arrest and DNA damage inducible gene (GADD45) and down-regulates bax in ES cell-derived neural progenitor cells.

Elf-EMF (50 Hz-Power line, 2 mT, 5 min.on/30min. off, Table 8) was applied for 6 or 48 hours on neural progenitors (Table 8). Semi-quantitative RT-PCR analysis revealed no effect of ELF-EMF on transcript levels of genes involved in neuronal differentiation (nurr1, en-1) and on markers of differentiating

(nestin) or differentiated neuronal (TH) or astrocytic (GFAP) cells. In addition, we studied the effect of ELF-EMF on transcript levels of genes involved in the regulation of cell homeostasis (hsp70), cell cycle (p21) and anti-apoptosis (bcl-2). RT-PCR analysis revealed that, whereas transcript levels of p21 and hsp70 remain similar in sham and ELF-EMF exposed variants, a significant up-regulation of the growth arrest inducible gene GADD45 was observed at stage 4d+11d. (Figure 39). The quantitative RT-PCR (Q-RT-PCR) with specific primers and TaqMan probes showed that bcl-2 was first down-regulated at stage 4+7d ($p<0.05$), then up-regulated in the intermediate stage 4+11d ($p<0.01$) and at the terminal stage 4+23d ($p<0.05$). GADD45 was significantly up-regulated at stage 4+11d, then down-regulated at the terminal stage 4+23d (Figure 40). These studies were further substantiated by immunofluorescence analyses of neuronal markers. However, by immunofluorescence analysis, no changes in intracellular distribution and number of cells expressing neuronal markers (β III-tubulin, TH, GFAP) were observed (data not shown).

Table 8. Conditions of the exposure of neuronal progenitor cells to ELF-EMF and summary of the effects on transcript abundance, neural differentiation induction and DNA break induction.

Intermittent exposure (5min on/30 min off)			
48 hours, ELF-EMF (Power line, 50Hz)		6 hours, ELF-EMF (Power line, 50Hz)	
2.0 mT	up-regulation followed by down-regulation of GADD45 up-regulation of bcl-2 down-regulation of bax no effect on neural differentiation no effect on DNA break induction (n=6)	2.0 mT	no effect on DNA break induction (n=3)

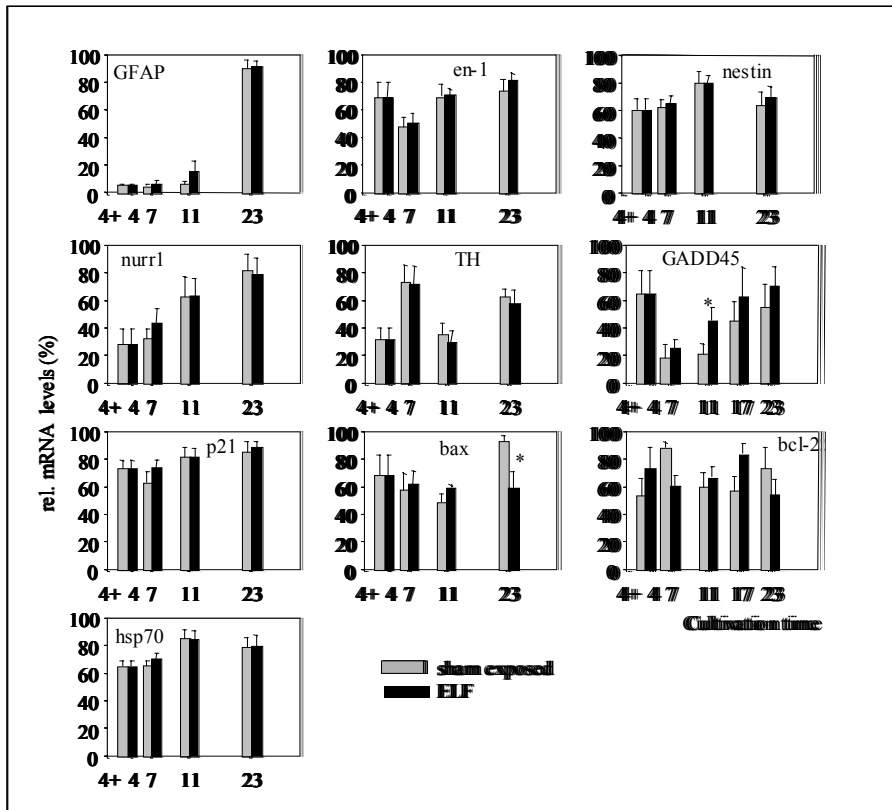


Figure 39. Relative mRNA levels of genes encoding the regulatory genes bcl-2, bax, p21, hsp70 and the genes involved in neuronal differentiation en-1, nurr1, TH, GFAP and nestin in ES-derived neural progenitors after 48 hours ELF (50Hz Powerline) EMF exposure (2.0 mT, intermittence 5 min ON/30 min OFF), at stage 4+4d - 4+6d. EMF exposure resulted in a significant transcript up-regulation of GADD45 and down-regulation of bax. Error bars represent standard deviations. Statistical significance was tested by the Student's t-test for a significance level of 5% (*, p < 0.05).

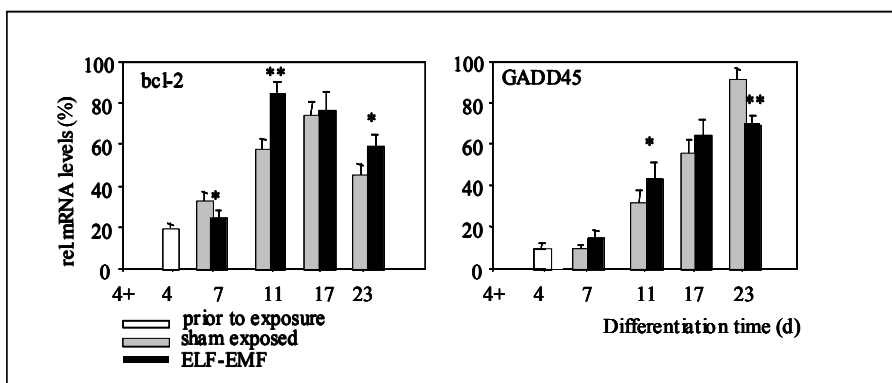


Figure 40.: Quantitative RT-PCR for estimation of relative mRNA levels of genes encoding the regulatory genes bcl-2 and GADD45 in ES-derived neural progenitors after 48 hours ELF (50Hz Powerline) EMF exposure (2.0 mT, intermittence 5 min on/30 min off), at stage 4+4d - 4+6d. EMF exposure resulted in a significant transcript down-regulation followed by up-regulation of bcl-2, which correlated with up-regulation followed by down-regulation of GADD45. Error bars represent standard deviations. Statistical significance was tested by the Student's t-test for a significance level of 5% and 1% (*, p < 0.05 ; **, p < 0.01).

3.1.4.2 Human neuroblastoma cell line SY5Y (Participant 11)

In order to obtain cellular models to study ELF-EMF, we have characterised some neuroblastoma cell lines for their ability to express nAChRs and evaluate whether ELF-EMF can interfere with the expression of alpha3, alpha5 and alpha7 nAChR subunits, as well as with that of Phox2a, Phox2b and dopamine-beta-hydroxylase (DβH).

Three human neuroblastoma cell lines (SH-SY5Y, SK-N-BE and IMR32) have been analysed, by means of northern blot analysis, for the expression of neuronal acetylcholine receptor subunits. Due to the high degree of homology between different subunits, the experiments have been carried out with probes derived from the cytoplasmic portion, the least conserved region of nAChR subunits, in order to avoid cross-contamination. The results showed that these cells express the ganglionic type of nAChRs (alpha3, alpha5 and alpha7), but not alpha 4, mainly expressed in the CNS (data not shown and Fornasari 1997; Flora 2000). Furthermore only human neuroblastoma cell lines SY5Y and IMR-32 appeared to express either Phox2a, Phox2b or DβH (Flora, 2001 and data not shown), although with differences in the level of expression. As the SY5Y lineage shows higher expression of the three genes, we decided to use this as a model in all the experiments.

ELF-EMF did not affect the expression of nicotinic acetylcholine receptors (nAChRs) which represent the neuronal nicotinic system in human neuroblastoma cells.

At the beginning of our experiment we decided to use field strengths which are larger than the maximum real-world exposure and eventually scale-down, in the case of measurable effect, establishing the minimum threshold level to which ELF-EMF do not represent a risk to human health. Neuroblastoma cell line SY5Y was then exposed to ELF-EMF (50 Hz, powerline signal) continuously for 16 hours at flux densities of 2 mT and 1 mT and the expression level of human alpha 3, alpha 5 and alpha 7 nAChRs subunits analysed by means of Northern blotting. Figure 41 (panel A) shows the results obtained by three independent exposures at 2 mT (lanes 1, 4 and 5) together with that of sham-exposed cells (lanes 2, 3 and 6). The densitometric quantification of the mRNA level, however, has shown no effect on the expression level of nAChR subunits as compared to that of the sham-exposed cells set as 100%, when cells were exposed either at 2 mT or 1 mT (Figure 41), panel B and C respectively). We then decided to explore whether an intermittent exposure might be influent on the expression of the nAChR subunits tested. Exposing the cells to intermittent magnetic field (5 min on/5 min off), 2 mT and 1 mT flux density, for 16 hours did not affect the expression of the alpha3, alpha5 and alpha7 nAChR subunit genes (Figure 42, panel A and B respectively).

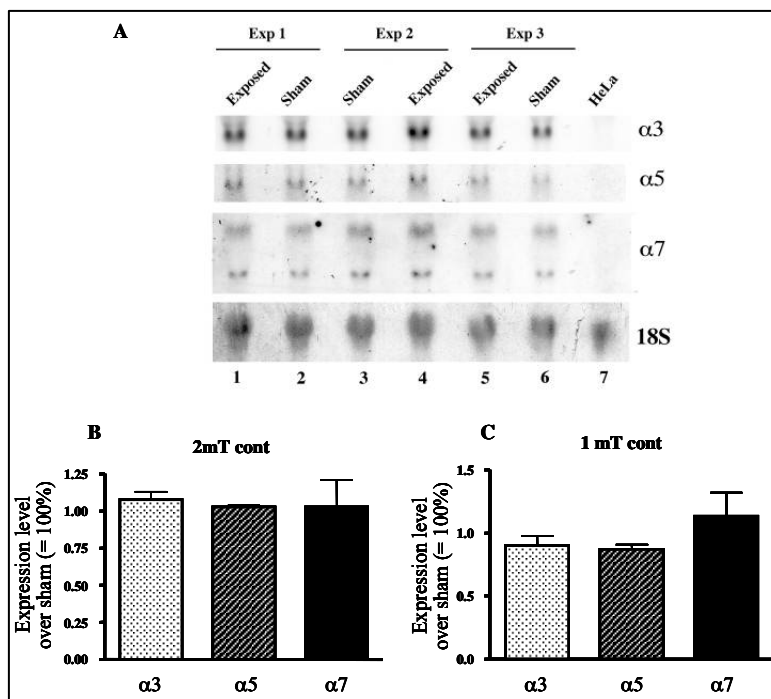


Figure 41. nAChR subunits expression upon exposure to 16 hours continuous ELF-EMF. 20 μ g of total RNA extracted from SY5Y cells exposed to 2mT and 1 mT continuous 50 Hz magnetic field, for 16 hours, was hybridised to cDNA probes corresponding to the human alpha3, alpha5 and alpha7 nAChR subunits. The expression level was normalised to that of 18S RNA. A, Northern blot analysis of total RNA extracted upon exposure to 2mT ELF-EMF. Here reported are the results of three independent experiments (Exp1, lanes 1-2; Exp 2, lanes 3-4; Exp 3, lanes 5-6). Lane 7, HeLa total RNA has been used as a negative control. B and C, Densitometric quantification of the expression level of nAChR subunits upon exposure to 2 mT and 1 mT continuous ELF-EMF, respectively. The data are the mean of three independent experiments \pm S.E., expressed as a percentage of the sham-exposed sample set equal to 100%.

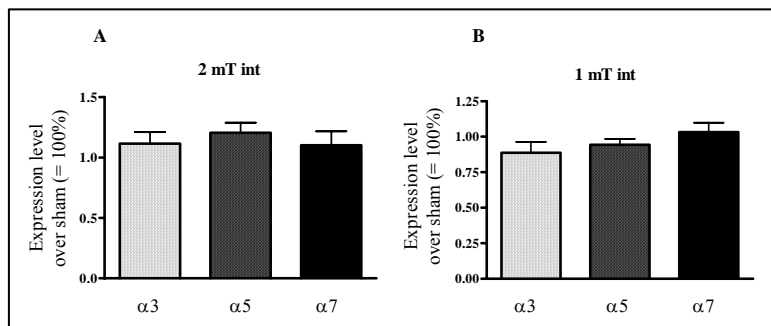


Figure 42. nAChR subunits expression upon exposure to 16 hours intermittent ELF-EMF. 20 μ g of total RNA extracted from SY5Y cells exposed to 2mT and 1 mT continuous 50 Hz magnetic field, for 16 hours, was hybridised to cDNA probes corresponding to the human alpha3, alpha5 and alpha7 nAChR subunits. The expression level was normalised to that of 18S RNA. The data are the mean of three independent experiments \pm S.E., expressed as a percentage of the sham-exposed sample set equal to 100%. A, Densitometric quantification of the expression level of nAChR subunits upon exposure to 2 mT intermittent ELF-EMF. B, Densitometric quantification of the expression level of nAChR subunits upon exposure to 1 mT intermittent ELF-EMF.

As we were not able to measure any effect at the mRNA level, we wondered whether the exposure to ELF-EMF might have an effect at the level of receptor proteins. To this purpose we carried out radioligand assays on cells exposed to either continuous or intermittent 50 Hz ELF-EMF, flux densities of 1 mT and 2 mT for 16 hours, to assess the amount of protein functionally assembled in the receptors. The

binding was performed in the presence of radiolabelled ligands, ^3H -Epibatidine to quantitate alpha3-containing receptor and ^{125}I -alpha-bungarotoxin to quantitate alpha7-containing receptor. However, as shown in Figure 43, no change in the amount of either alpha3- or alpha7-containing receptor was detected under the same conditions used in Northern blot analysis of Figures 41 and 42, as compared to that of the sham-exposed cells set as 100%.

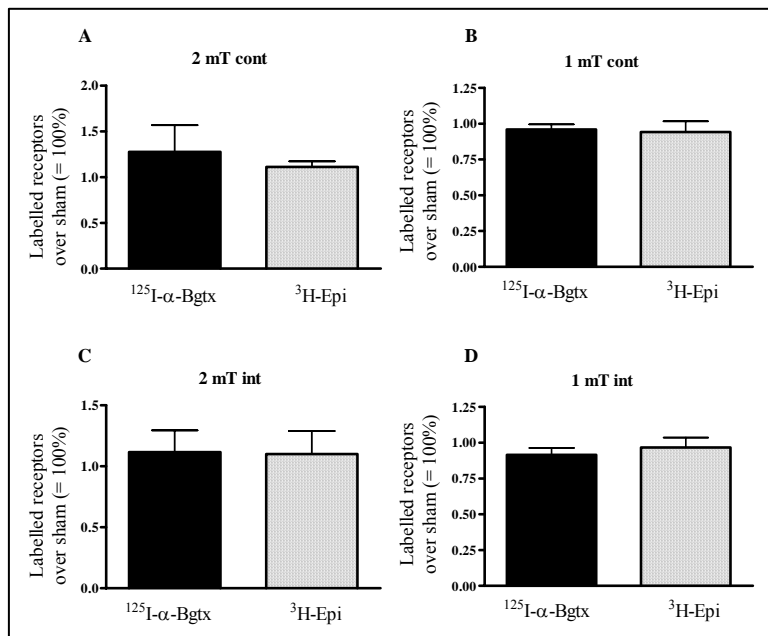


Figure 43. Quantitative analysis of the alpha3- and alpha7-containing receptors upon continuous and intermittent ELF-EMF exposure for 16 hours

The amount of labelled receptors were obtained from the binding of saturating concentration of ^3H -Epibatidine (grey bars) and ^{125}I -alpha-bungarotoxin (black bars) to the cell homogenates, performed in quadruplicate. The values are the mean of three independent experiments \pm and S.E. are expressed as percentage of labelled receptors in the exposed samples with respect to the sham-exposed cells set as 100%. A and B, continuous exposure to 1 mT and 2 mT ELF-EMF, respectively. C and D, intermittent (5 min on/5 min off) exposure to 1 mT and 2 mT ELF-EMF.

The experiments carried out until now have showed that the ELF-EMF does not influence the expression of nAChRs upon exposure of the cells to magnetic field with flux densities of either 1 mT or 2 mT for a relatively short period of time (16 hours). We then investigated whether the duration time of the exposure of SY5Y cells to ELF-EMF might affect the expression of the genes encoding the nAChR subunits, and especially, whether longer exposure to ELF-EMF might affect the expression of some of the genes. To answer this question two different exposure protocols have been used: a) 50 Hz powerline signal, flux density 1 mT, continuous exposure, duration 48 hours. The RNA or proteins were extracted immediately after the end of exposure (immediate recovery); b) 50 Hz powerline signal, flux density 1 mT, continuous exposure, duration 48 hours. The RNA or proteins were extracted 48 hours after the end of exposure (delayed recovery).

As shown in Figure 44, panel A, the expression of nAChR subunits, as measured at mRNA level, was again not affected by a prolonged exposure to the ELF-EMF followed by an immediate recovery of the cells (protocol a). Furthermore, no effect was detected at the level of receptor proteins (Figure 44, panel B). We then wondered whether the effect could be a delayed one, that is mediated by the activation of a cascade of second messengers that results in a change of gene expression. To test this hypothesis, cells were collected for RNA and protein analysis 48 hours after the end of the exposure (protocol b). The

results shown in Figure 44 seemed to rule out an indirect effect as neither the level of mRNA (Figure 45, panel A) nor of the receptor proteins (Figure 45, panel B) changed under these experimental conditions.

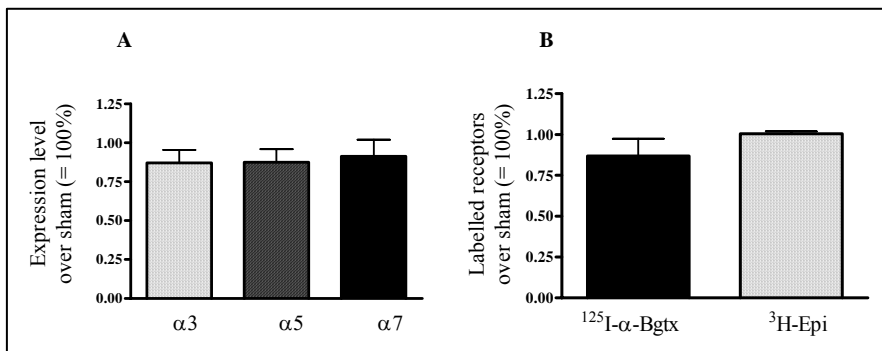


Figure 44. nAChR subunits expression and quantitative analysis of the alpha3- and alpha7 containing receptors upon continuous exposure to 1 mT ELF-EMF for 48 hours: Immediate recovery

Cells were exposed to 1 mT ELF-EMF for 48 hours and recovered immediately after the end of the exposure. A, Densitometric quantification of the expression level of nAChR subunits after Northern blot analysis. The data are the mean of five independent experiments \pm S.E., expressed as a percentage of the sham-exposed sample set as 100%. B, quantification of the alpha3- (grey bars) and alpha7-containing (black bars) receptors. The values are the mean of three independent experiments \pm and S.E. are expressed as percentage of labelled receptors in the exposed samples with respect to the sham-exposed cells set as 100%.

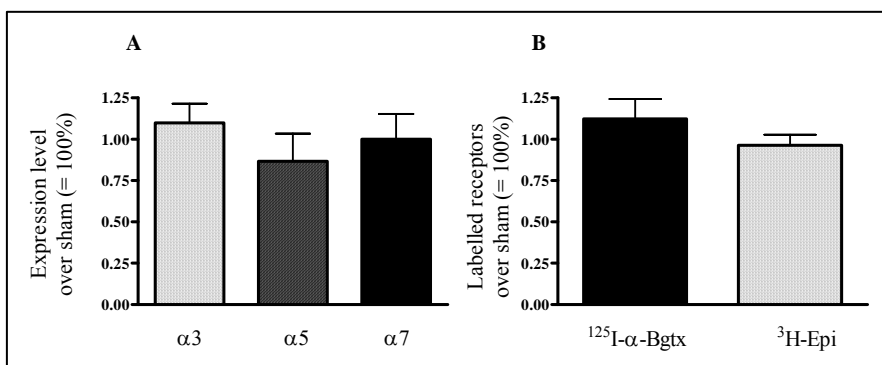


Figure 45. nAChR subunits expression and quantitative analysis of the alpha3- and alpha7 containing receptors upon continuous exposure to 1 mT ELF-EMF for 48 hours: Delayed recovery

Cells were exposed to 1 mT ELF-EMF for 48 hours and recovered 48 hours after the end of the exposure. A, Densitometric quantification of the expression level of nAChR subunits after Northern blot analysis. The data are the mean of five independent experiments \pm S.E., expressed as a percentage of the sham-exposed sample set as 100%. B, quantification of the alpha3- (grey bars) and alpha7-containing (black bars) receptors. The values are the mean of three independent experiments \pm and S.E. are expressed as percentage of labelled receptors in the exposed samples with respect to the sham-exposed cells set as 100%.

ELF-EMF did not affect the expression of markers of the catecholaminergic system in neuroblastoma cells.

In collaboration with Participant 1 we decided to investigate the influence of ELF-EMF on neurotransmitter release. In particular, the activity of the dopamine-beta-hydroxylase (D β H) which is a key enzyme in the synthesis of noradrenaline has been studied. Furthermore, we investigated possible modifications on the expression of two related homeo-domain transcription factors, Phox2a and Phox2b, that are relevant for the specification of the autonomic nervous system. Moreover, in noradrenergic cells, they are directly involved in the determination of the neurotransmitter phenotype by regulating the expression of D β H. As protocols, we applied the same exposure conditions used for the analysis of the human nAChR subunits. As shown in Figure 46, panels A and B, continuous exposure of SY5Y neuroblastoma cells to 1 mT and 2 mT 50 Hz ELF-EMF did not affect the expression level of either Phox2a, Phox2b and D β H genes, as compared to that of the sham-exposed cells set to 100%. Again we asked whether an intermittent exposure might have an effect on gene expression of these proteins. We then measured the mRNA level upon intermittent exposure (5 min on/5 min off) to 1 mT ELF-EMF, but no change was observed (Figure 47). Previous experiments have shown that an exposure of SY5Y cells for 48 hours at 1 mT flux density reduced the amount of mRNA of Phox2a, but not of Phox2b and D β H. We then exposed the cells under these conditions up to nine times independently.

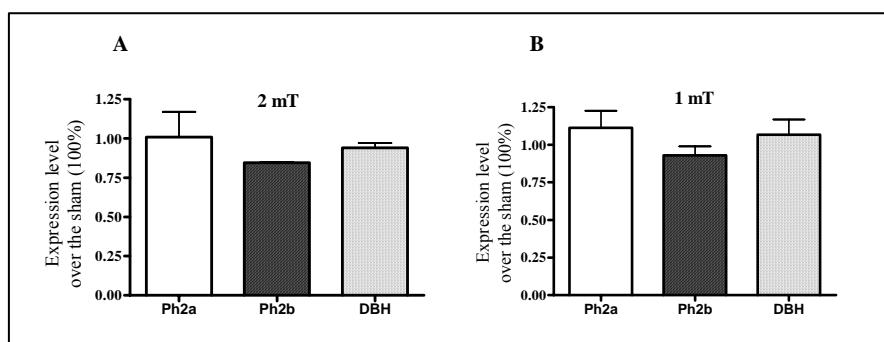


Figure 46. Noradrenergic phenotype specifying genes expression upon continuous exposure to ELF-EMF for 16 hours

20 μ g of total RNA extracted from SY5Y cells continuously exposed to 1mT and 2 mT 50 Hz ELF-EMF for 16 hours was hybridised to cDNA probes corresponding to the human Phox2a, Phox2b and D β H genes. The expression level was normalised to that of 18S RNA. A Densitometric quantification of the expression level of the three genes upon continuous exposure to 2 mT ELF-EMF. B, Densitometric quantification of the expression level of the three genes upon continuous exposure to 1 mT ELF-EMF. The data are the mean of five independent experiments \pm S.E., expressed as a percentage of the sham-exposed sample set as 100%.

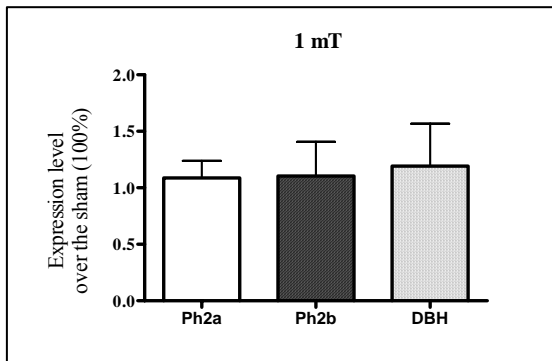


Figure 47. Noradrenergic phenotype specifying genes expression upon intermittent exposure (5 min on/5 min off) to ELF-EMF for 16 hours.

Densitometric quantification of the expression level of the three genes upon intermittent exposure to 1 mT ELF-EMF, after Northern blot analysis. The data are the mean of five independent experiments \pm S.E., expressed as a percentage of the sham-exposed sample set as 100%.

Statistical analysis has ruled out that, upon this exposure protocol, the expression of the noradrenergic specifying genes was affected, as shown in Figure 48, either harvesting the cells immediately after the end of the exposure (Figure 48, panel A) or 48 hours later (Figure 48, panel B). As no change was seen at the level of mRNA we asked whether the exposure to ELF-EMF might affect the expression of Phox2a and Phox2b at protein level. To this purpose we decided to measure, by western blot analysis, the protein level upon continuous exposure to 50 Hz ELF-EMF, flux density 1 mT, for 16 and 48 hours (Figure 49). Cells were harvested immediately after the end of the exposure (Figure 49, lanes 10-13 and lanes 6-9, respectively). Also protein extract from cells harvested 48 hours after the end of the continuous 48 hours exposure was tested (Figure 49, lanes 2-5). Densitometric analysis of the signal obtained for Phox2a (Figure 49, panel A) and Phox2b (Figure 49, panel B), normalised to that of the beta-tubulin, revealed that exposure of SY5Y cells to relatively short or longer period of time did not affect the expression of Phox2a and 2b, at protein level, as compared to that of the sham-exposed cells (Figure 49, panel C).

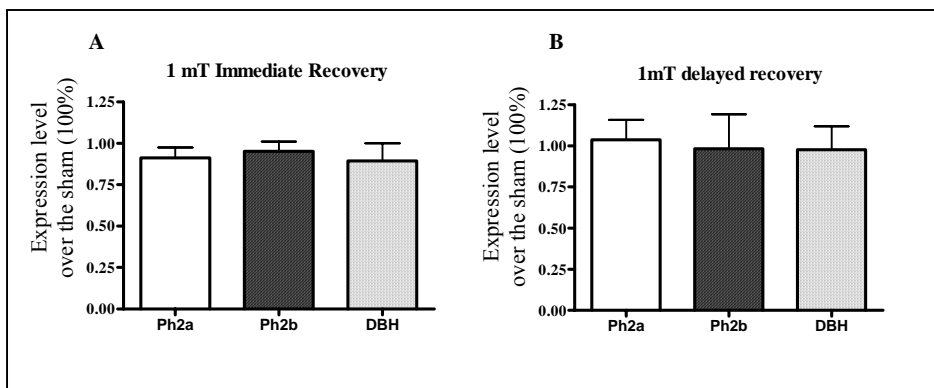


Figure 48. Noradrenergic phenotype specifying genes expression upon continuous exposure to ELF-EMF for 48 hours

SY5Y cells were continuously exposed to 1 mT 50 Hz ELF-EMF for 48 hours and collected either immediately (panel A) or 48 hours (panel B) after the end of the exposure. After northern blot analysis, the expression level of Phox2a, Phox2b and D β H genes was quantified by densitometric scanning of the autoradiogram. The data are the mean of six independent experiments \pm S.E. (Phox2b and D β H) and nine independent experiments (Phox2a), expressed as a percentage of the sham-exposed sample set equal to 100%.

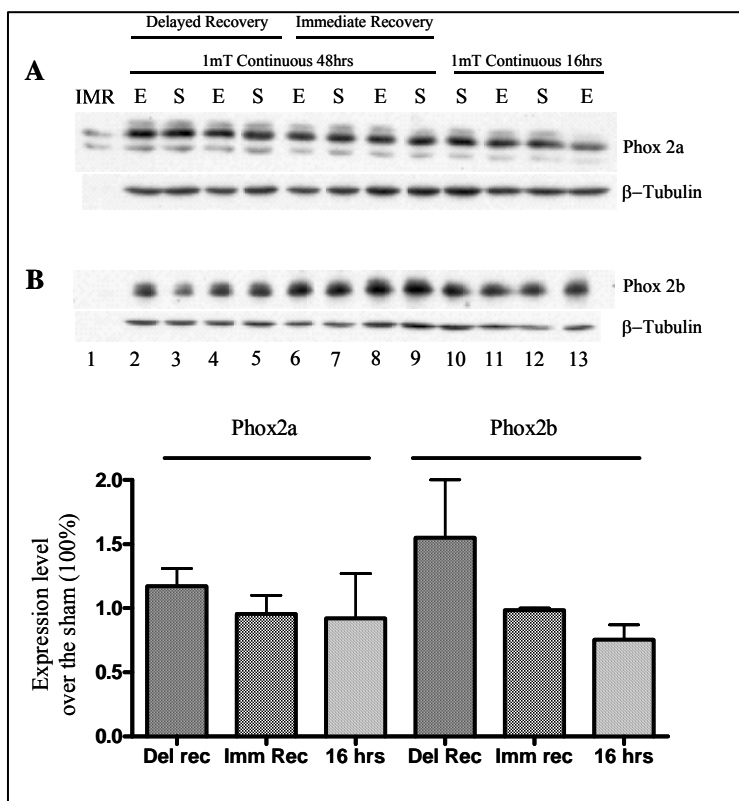


Figure 49. Western blot analysis of Phox2a and Phox2b expression upon continuous exposure to 1 mT ELF-EMF. 20 µg of total protein extract were size-fractionated by SDS-PAGE and transferred to nitrocellulose membrane. The expression of Phox2a and Phox2b was detected by incubation with anti-Phox2a (panel A) and anti-Phox2b antibodies (panel B). Lanes 2-9, samples from continuous exposure to 1 mT ELF-EMF for 48 hours recovered 48 hours (lanes 2-5) or immediately (lanes 6-9) after the end of the exposure. Lanes 10-13, samples from 1 mT continuous exposure for 16 hours. Lane 1, IMR 32 neuroblastoma cells nuclear extract used as a control. E= exposed, S= sham-exposed. The expression of Phox2a and Phox2b was normalised to that of β-tubulin. C, quantification of the expression level of Phox2a and Phox2b. The data are the mean of two independent exposures ± S.E. and are expressed as percentage of the sham-exposed samples set as 100%. Del Rec = recovery 48 hours after the end of the exposure; Imm rec = recovery immediately after the end of the exposure; 16 hours = samples were exposed for 16 hours to 1 mT continuous ELF-EMF.

3.1.4.3 Embryonic stem cells of mice during cardiac differentiation (Participant 8)

In higher vertebrates, heart formation is a complex phenomenon that starts at early stages of embryogenesis, prior to the end of gastrulation, with commitment of anterior lateral plate mesoderm cells to cardiogenic lineage. Studies in different organ systems have shown that tissue-specific transcription factors which control the expression of differentiation markers are also regulators of cellular differentiation. Basic helix-loop-helix proteins such as the myogenic factor are key regulators of skeletal muscle differentiation, while the erythroid cell-specific zinc finger protein GATA-1 is crucial for erythroid cell differentiation. It is now becoming evident that inactivation of the mouse homologue of the *Drosophila melanogaster* homeobox gene *tinman*, the homeobox gene *Nkx2.5* or *Csx* affects heart morphogenesis (Biben 1997, Lints 1993). Moreover, the GATA-4 protein, a member of the GATA family of transcription factors, has been found to be restricted to the hearts and to characterise very early stages of heart formation during embryonic development (Grepin 1995).

ELF-EMF affected the expression of cardiogenic genes in murine embryonic stem cells (GTR1).

In the first step of our study we looked at the effects of ELF-EMF (0.8 mT, 50 Hz sinusoidal) on the expression of cardiogenic genes in mouse embryonic carcinoma (EC) cells (P19 cells). Despite the encouraging results obtained in our pilot experiments, in a subsequent set of ten separate experiments P19

cells exposed to ELF-EMF desultorily underwent a gene program of cardiogenesis and revealed structural and functional cardiomyocyte features. Only in 2 experiments, exposure to ELF-EMF primed the expression of both GATA-4 and Nkx-2.5 genes, and led to the appearance of alpha-myosin heavy chain (MHC) and myosin light chain-2V (MLC), two cardiospecific transcripts. A representative RT-PCR analysis of cardiogenic and cardiac specific gene expression from ELF-EMF responsive cells is shown in Figure 50).

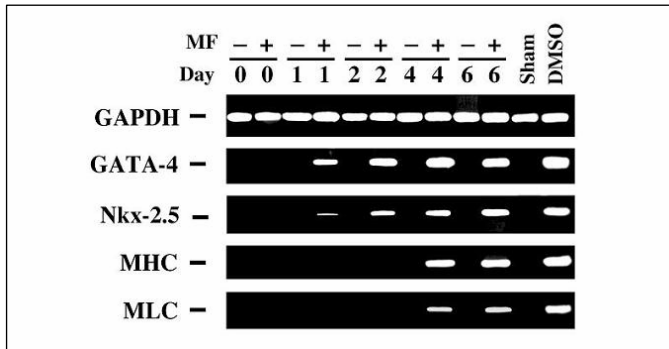


Figure 50. RT-PCR analysis of cardiogenic and cardiospecific transcripts in P19 cells exposed to ELF-EMF (continuous exposure, 4 days). MHC, alpha-myosin heavy chain. MLC, myosin light chain-2V.

We reasoned that the lack of data reproducibility of these results could be due to the consistent dilution of the myocardial phenotype within multiple non-myocardial cells encompassed by the P19 model of cell differentiation. To circumvent this problem, we decided to change the biological model, by using a line of pluripotent embryonic stem (ES) cells engineered for a gene trapping selection of a virtually pure population of ES-derived cardiomyocytes. RT-PCR analysis of targeted transcripts in unexposed cells indicated that, differently from undifferentiated LIF-supplemented cells, EBs expressed both GATA-4 and Nkx-2.5 mRNA (Figure 51). The expression of these cardiogenic genes resulted to be further enhanced in puromycin selected, ES-derived cardiomyocytes (Figure 52). Figures 51 and 52 show that ELF-EMF exposure remarkably increased GATA-4 and Nkx-2.5 gene expression in both EBs and cardiomyocytes, as compared to unexposed GTR1 cells. Interestingly, in both groups of cells ELF-EMF also increased the expression of the prodynorphin gene, an endorphin gene that has been recently shown to play a major role in orchestrating ES cell cardiogenesis (Ventura 2003(a), 2003(b), 2000). These responses were further inferred by the quantitative analysis of mRNA levels as shown in RNase protection experiments (Figure 53). Interestingly, nuclear run-off analyses of GATA-4 gene transcription indicated that the ELF-EMF action occurred at the transcriptional level (Figure 54). The activation of a program of cardiogenic gene transcription was also associated with the appearance of the cardiac specific transcripts alpha-myosin heavy chain and myosin light chain-2V (Figure 55).

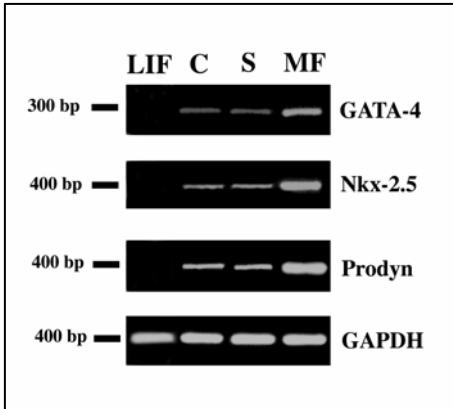


Figure 51. ELF-EMF was applied from the time of LIF removal and EBs were collected after 3 additional days. C: control EBs; S: sham. (Ethidium bromide-stained agarose gels, representative of 4 separate experiments).

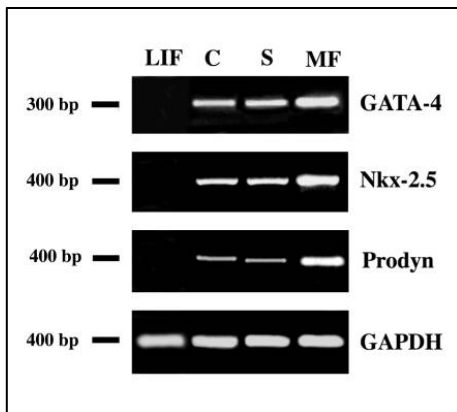


Figure 52. Effect of ELF-EMF (MF) on Cardiogenic gene expression in puromycin-selected cells. ELF-EMF was applied from the time of LIF removal throughout puromycin selection. Four days after puromycin addition (10 days from LIF withdrawal), ES-derived cardiomyocytes were processed gene expression analyses. C: control puromycin-selected cardiomyocytes; S: sham. (Ethidium bromide-stained agarose gels, representative of 4 separate experiments).

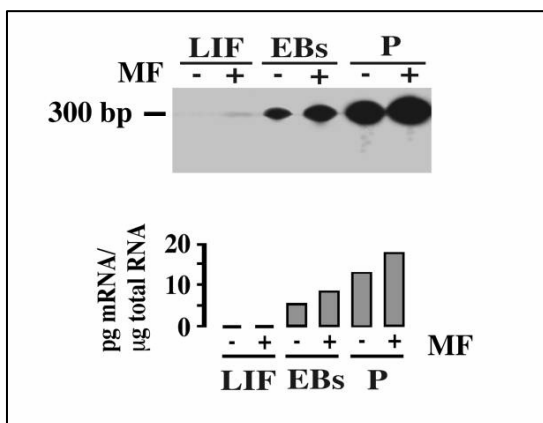


Figure 53. RNase protection analysis of GATA-4 mRNA expression in GTR1 ES cells cultured in the absence or presence of ELF-EMF. LIF, undifferentiated GTR1 cells. EBs, embryoid bodies collected 5 days after LIF removal. P, puromycin-selected cardiomyocytes: puromycin was added at day 8 following LIF removal. Each group of cells was cultured in the absence (-) or presence (+) of ELF-EMF. Autoradiograms are representative of 3 separate experiments.

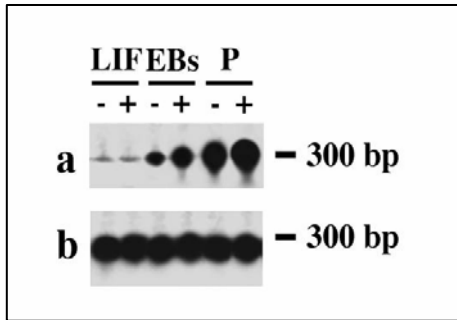


Figure 54. Nuclear run-off analysis of GATA-4 gene transcription in isolated ES cell nuclei. Nuclei were isolated from undifferentiated GTR1 cells (LIF), from EBs collected 5 days after LIF removal (EBs) or from puromycin-selected cardiomyocytes (P): puromycin was added at day 8 following LIF removal. Each group of cells was exposed in the absence (-) or presence (+) of ELF-EMF (MF). Puromycin was added at day 8 following LIF removal. Row a, GATA-4 gene transcription. Row b, cyclophilin gene transcription (cyclophilin was assessed as a constant gene for control). Autoradiograms are representative of 3 separate experiments.

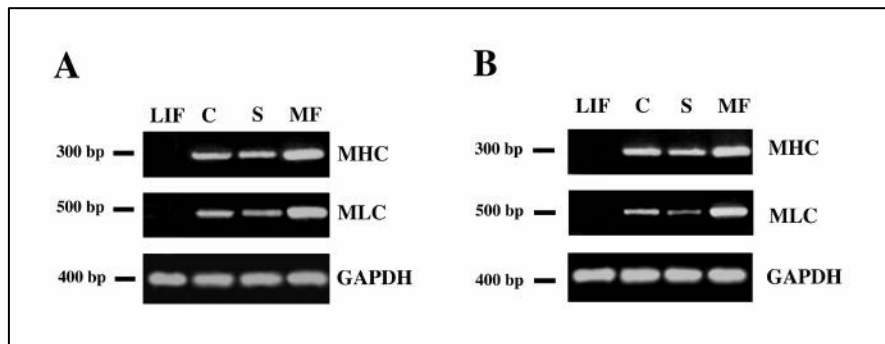


Figure 55: Effect of MF on the expression of cardiac specific genes. A: ELF-EMF (MF) was applied from the time of LIF removal and EBs were collected after additional 3 days. B: MF was applied from the time of LIF removal throughout puromycin selection. Four days after puromycin addition (10 days from LIF withdrawal), ES-derived cardiomyocytes were processed gene expression analyses. C: control cells; S: sham. (Ethidium bromide-stained agarose gels, representative of 4 separate experiments).

Exposure of GTR1 ES cells to ELF-EMF after LIF removal and throughout 4 days of puromycin selection for an overall period of 10 days from LIF withdrawal was able to increase the yield of ES-derived cardiomyocytes: the number of beating colonies reached 170.44 ± 28.0 % of the control value, estimated in cardiomyocytes selected from untreated cells (mean \pm SEM of 4 separate experiments).

We finally investigated whether the transcriptional responses evoked by ELF-EMF may encompass genes that are essential for the specification of non-myocardial lineages. Noteworthy, the expression of MyoD, a gene involved in skeletal myogenesis was not affected in both EBs and puromycin selected cells (Figure 56), while the expression of neurogenin1, a neuronal specification gene, was slightly enhanced only in EBs (Figure 56).

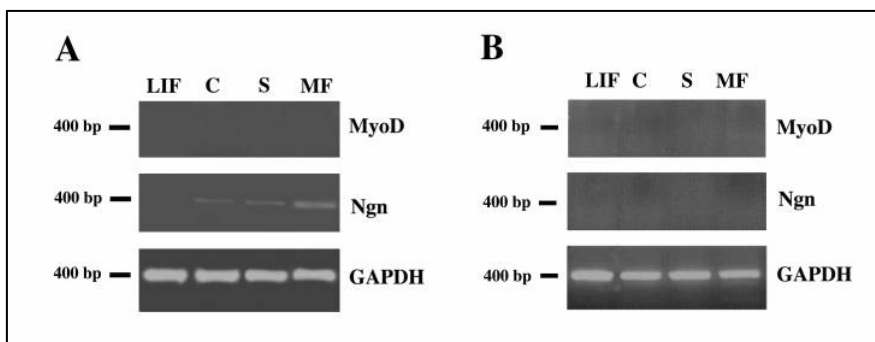


Figure 56. Effect of ELF-EMF (MF) on the expression of genes promoting non-myocardial lineages. A: MF was applied from the time of LIF removal and EBs were collected after additional 3 days. B: MF was applied from the time of LIF removal throughout puromycin selection. Four days after puromycin addition (10 days from LIF withdrawal), ES-derived cardiomyocytes were processed gene expression analyses. C: control cells; S: sham. MyoD and neurogenin1 (Ngn) are skeletal muscle and neuronal specification genes, respectively. (Ethidium bromide-stained agarose gels, representative of 4 separate experiments).

3.1.4.4 Membrane currents of oocytes of *Xenopus laevis* expressing rCx46 (Participant 7)

ELF-EMF did not significantly affect the leak-current of oocytes of Xenopus laevis expressing hemi-channels of rCx46.

During expression of hemi-channels, composed of the connexin rCx46, the oocytes were exposed to ELF-EMF (50 Hz). As suitable parameter for functional integrity of an oocyte the leak-current was selected which was electrophysiologically measured at voltage-clamp. A representative experiment of a sham exposed oocyte is shown in Figure 57. Figure 57a) shows membrane currents recorded at depolarising test potentials starting from a holding potential of -90 mV. The figure indicates that the rCx46-mediated current becomes activated by depolarising test potentials above about -10 mV. Figure 57b) shows the corresponding leak subtracted steady-state current values (I_{ss}) as function of driving voltage ($V-V_{rev}$) where V_{rev} denotes the corresponding reversal potential. The corresponding steady-state current values were derived at the end of the applied test pulse.

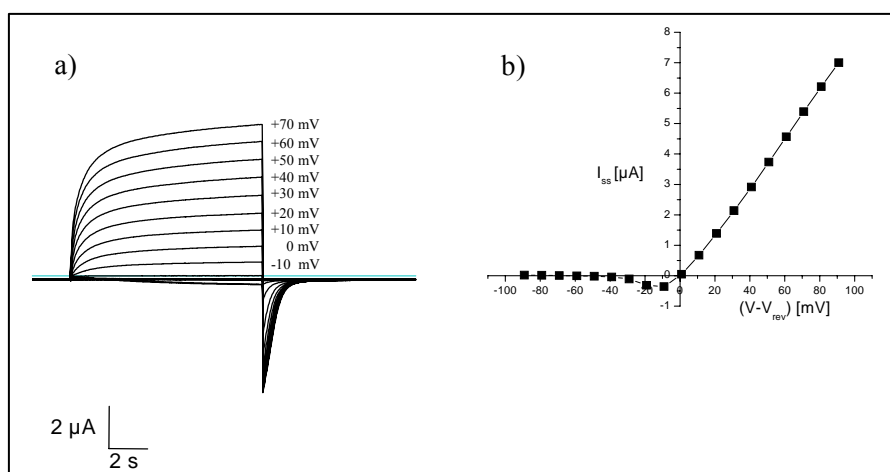


Figure 57. Voltage-dependent current activation of sham exposed *Xenopus* oocytes expressing rCx46 after an expression time of 16 hours. **a)** Representative voltage-jump current-relaxations at given test potentials. The common holding potential was set to -90 mV. The dotted line denotes the zero current level. **b)** Leak subtracted steady-state current amplitudes (I_{ss} , ■) derived from the data in a) as function of driving voltage ($V-V_{rev}$)

The leak-current was derived at test potentials in the range of -70 mV to -100 mV using a constant holding potential of -90 mV. A comparison of leak-currents for exposed and sham exposed oocytes is given in Figure 58. Figure 58a shows the leak-current for oocytes which were continuously exposed for 16 hours at 2.3 mT and Figure 58b) the corresponding leak-current after an intermittent exposure (5 min on/10 min off) at 1.0 mT for 16h. A significant influence of ELF-EMF exposure on the leak current could not be observed for the different exposure conditions.

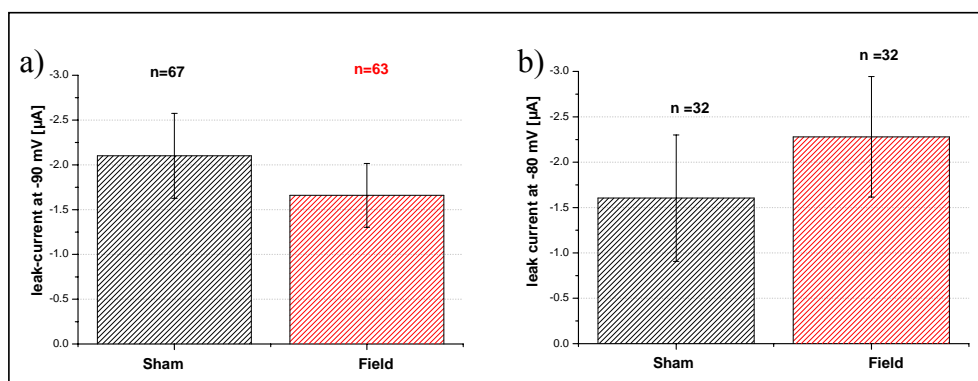


Figure 58. Leak-currents of single oocytes after expression of rCx46- hemi-channels at different holding potential. **a)** Leak current amplitudes at holding potential -90 mV of sham and ELF-EMF (2.3 mT, 16 hours) continuously exposed oocytes. **b)** Leak-currents at holding potential -80 mV of sham and ELF-EMF (1.0 mT, 16 hours, 5 min on/10 min off) exposed oocytes. Data are given as mean \pm s.e.m. n denotes the number of different oocytes.

No significant influence of ELF-EMF on the number of expressed and conducting hemi-channels composed of rCx46 in oocytes.

The expression level of hemi-channels composed of rCx46 was estimated from the number of conducting hemi-channels which corresponds to the mean steady-state current amplitude (I_{ss}) and/or the maximal membrane conductance G_{max} at depolarising test potentials. Expression of endogenous hemi-channels was suppressed by injection of the corresponding anti-sense. Figures 59a, 60a and 61a show the relationship I_{ss} vs $(V-V_{rev})$ for different oocytes for the selected exposure condition. For clearer presentation $G(V)$ was normalised to a maximal value of $G(V)$ which is obtained at $V = +50$ mV (Figures 59b, 60 and 61b). A significant influence of ELF-EMF exposure on the number of expressed and conducting hemi-channels of rCx46 could not be read from the analysed data. This finding is also reflected in the frequency distribution of G_{max} for sham and exposed oocytes (Figure 59c).

No significant influence of ELF-EMF on the voltage-dependent gating properties of rCx46 expressing oocytes

A possible effect of ELF-EMF exposure on the voltage dependent gating properties of conducting hemi-channels of rCx46 was analysed. I_{ss} vs $(V-V_{rev})$ was measured and the corresponding relation $G(V)$ vs $(V-V_{rev})$ derived. The latter relationship could be fitted by a simple Boltzmann equation. The fit yields as essential parameter the number of apparent equivalent voltage gating charges z . z was determined for the different exposure conditions. As can be read from Figure 59a) a significant effect of ELF-EMF exposure on the voltage-dependent gating which is reflected in the apparent number of equivalent charges z (Figure 59b) was not observed.

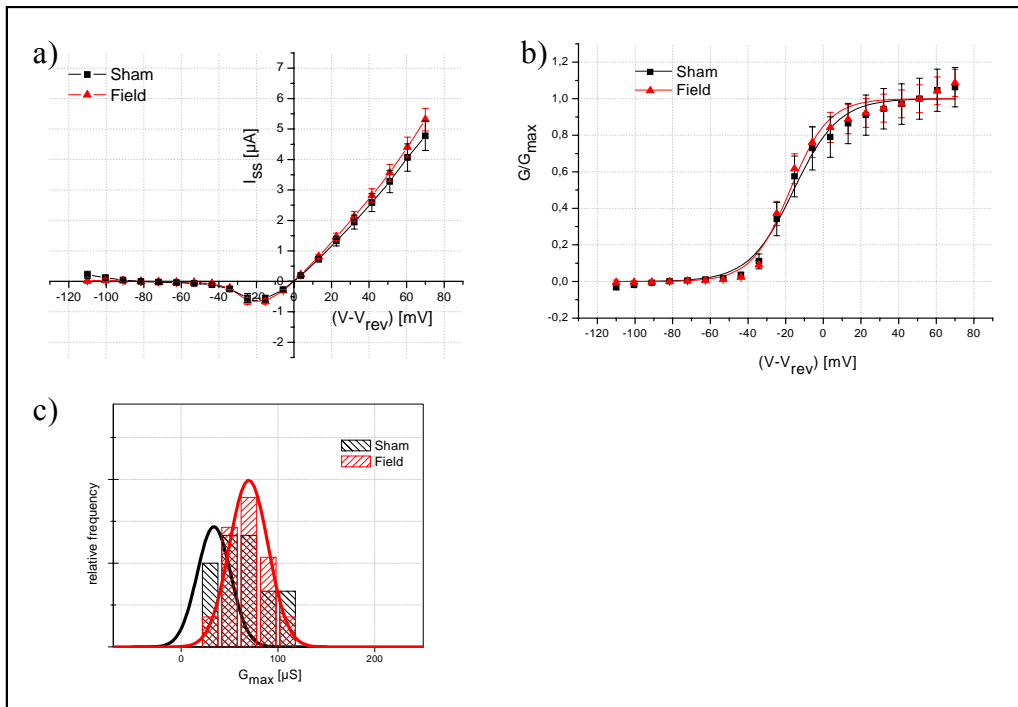


Figure 59. Voltage dependence of macroscopic rCx46-mediated membrane current and corresponding conductance after continuous ELF-EMF exposure for 16 hours at 2.3 mT. **a)** Mean \pm s.e.m. of leak subtracted steady-state current amplitudes (I_{ss}) as function of $(V-V_{rev})$ in the absence and presence of ELF-EMF exposure (sham \blacksquare , $n = 14$; field \blacktriangle , $n=15$). **b)** Mean \pm s.e.m. of corresponding normalised membrane conductance $G/G_{max} = G(V)/G(V=+50 \text{ mV})$ as function of $(V-V_{rev})$ in the absence (\blacksquare , $n = 14$) and presence of ELF (\blacktriangle , $n = 15$). The solid lines show fits of the data by a simple Boltzmann function (for details see Materials and Methods). The derived parameters are $z(\text{sham}) = 2.11 \pm 0.17$; $z(\text{field}) = 2.45 \pm 0.23$; $V_{1/2}(\text{sham}) = (-15.76 \pm 1.06) \text{ mV}$; $V_{1/2}(\text{field}) = (-17.66 \pm 1.07) \text{ mV}$. **c)** Distribution of relative frequency of $G_{max} = G(V=+50 \text{ mV})$ in the absence ($n = 14$) and presence ($n = 15$) of ELF-EMF. Solid lines present the Gauss distribution with the parameters: $G_{max, \text{mean}}(\text{sham})=64.2 \mu\text{S}$, corresponding standard deviation (sd) $\text{sd}(\text{sham}) = 7.8 \mu\text{S}$ and $G_{max, \text{mean}}(\text{field}) = 69.8 \mu\text{S}$, $\text{sd}(\text{field}) = 20.0 \mu\text{S}$

To investigate an influence of field intensity on the results presented above, the experiments were repeated at 1.0 mT and the EMF-ELF was intermittently applied (5 min on/10 min off) for 16 hours. The corresponding results are given in Figure 60. Again, a significant effect of ELF-EMF on the number of expressed hemi-channels of rCx46 (Figure 59a) as well as their voltage dependent gating properties was not observed (Figure 60b).

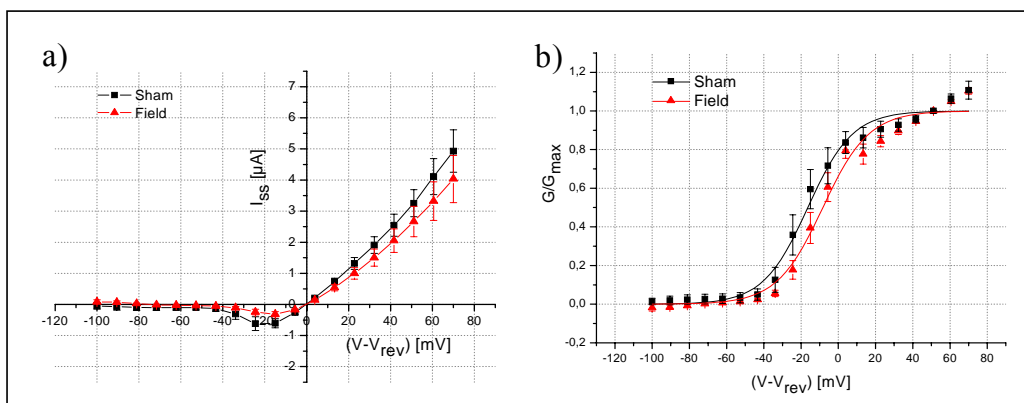


Figure 60. Voltage dependence of rCx46-mediated membrane currents and corresponding membrane conductance after intermittent ELF-EMF exposure (5 min on/10 min off) for 16 hours at 1.0 mT. **a)** Mean \pm s.e.m. of leak subtracted steady-state current amplitudes (I_{ss}) as function of ($V-V_{rev}$) in the absence and presence of ELF-EMF exposure (sham \blacksquare , $n = 5$; field \blacktriangle , $n = 5$). **b)** Mean \pm s.e.m. of normalised membrane conductance $G/G_{max} = G(V)/G(V = +50 \text{ mV})$ as function of driving voltage ($V-V_{rev}$) in the absence (\blacksquare , $n = 5$) and presence of ELF-EMF (\blacktriangle , $n = 5$). The solid lines present fits of the data by a simple Boltzmann function, respectively (for details see Materials and Methods). The derived parameters are $z(\text{sham}) = 2.08 \pm 0.19$; $z(\text{field}) = 2.02 \pm 0.20$; $V_{1/2}(\text{sham}) = (-16.39 \pm 1.29) \text{ mV}$; $V_{1/2}(\text{field}) = (-8.32 \pm 1.38) \text{ mV}$

In a further series of experiments ELF-EMF at an intensity of 2.3 mT was intermittently (5 min on/10 min off) applied for 16 hours. The corresponding results are given in Figure 61. A significant effect of ELF-EMF exposure on the number of expressed hemi-channels of rCx46 (Figure 61a) was not observed. The data indicate a decrease of z after ELF-EMF exposure which appears not be significant (see legend of Figure 61b).

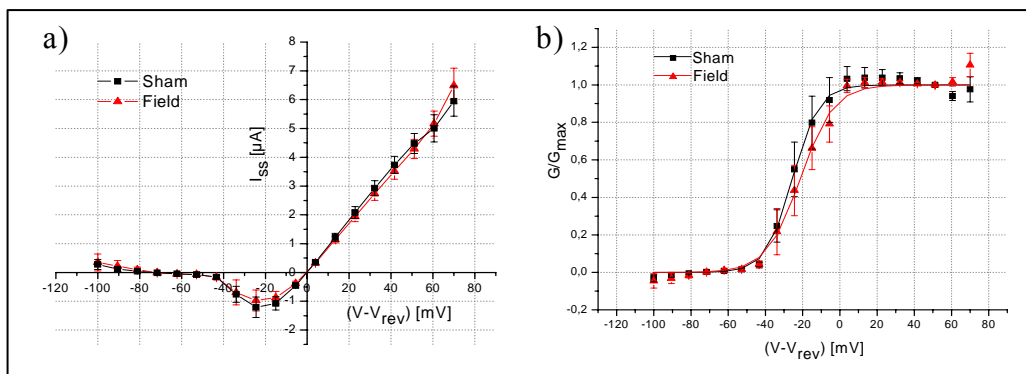


Figure 61. Voltage dependence of macroscopic rCx46-currents (I_{ss}) and corresponding membrane conductance (G) after intermittent exposure (5 min on/10 min off) for 16 hours at 2.3 mT. **a)** Mean \pm s.e.m. of leak subtracted steady-state current amplitudes (I_{ss}) as function of ($V-V_{rev}$) in the absence and presence of ELF-exposure (sham \blacksquare , $n = 4$; field \blacktriangle , $n = 5$). **b)** Mean \pm s.e.m. of normalised membrane conductance $G/G_{max} = G(V)/G(V = +50 \text{ mV})$ as function of ($V-V_{rev}$) in the absence (\blacksquare , $n = 4$) and presence of ELF-EMF (\blacktriangle , $n = 5$). The solid lines show fits of the data by a simple Boltzmann function (see Material and Methods). The derived parameters are $z(\text{sham}) = 3.54 \pm 0.26$; $z(\text{field}) = 2.77 \pm 0.24$; $V_{1/2}(\text{sham}) = (-25.51 \pm 0.59) \text{ mV}$; $V_{1/2}(\text{field}) = (-21.31 \pm 0.88) \text{ mV}$

For a more detailed analysis of the voltage dependent gating properties the kinetics of rCx46-mediated current activation was considered. The time dependent current activation could be described by a sum of two exponential functions: $I(t) = a_0 + a_1 \cdot \exp(1 - \exp(-t/\tau_1)) + a_2 \cdot \exp(1 - \exp(-t/\tau_2))$. The corresponding time constants of activation τ_1 and τ_2 were obtained from corresponding fits to the experimental data and the

results are presented in Figures 62a-c. The figure indicates that ELF-EMF exposure does not influence the voltage dependent time constants of channel activation significantly.

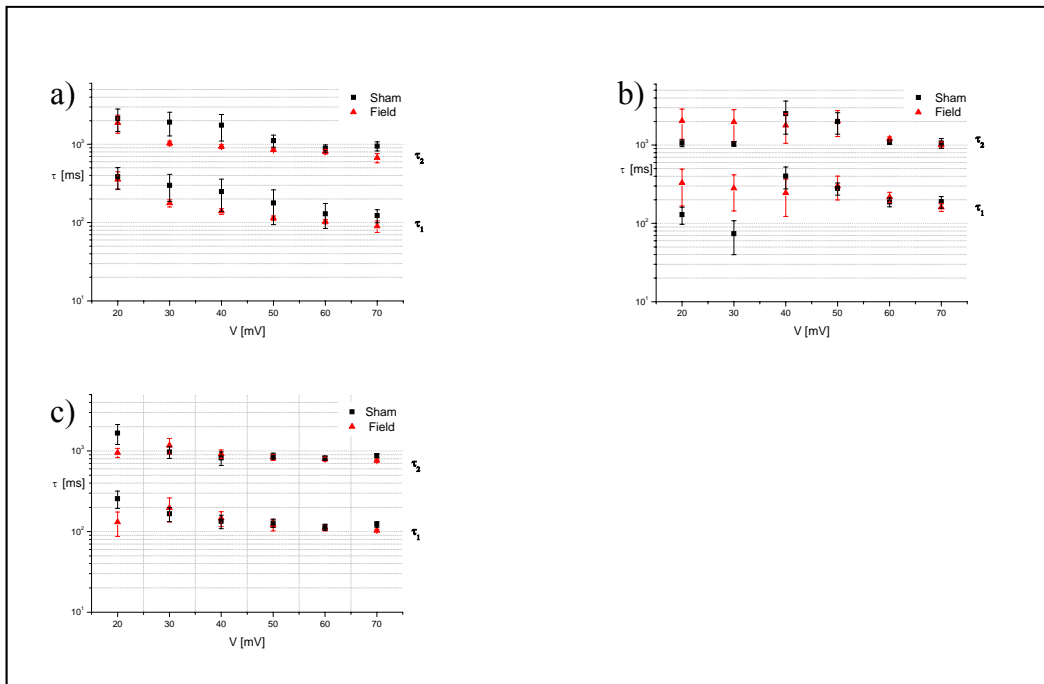


Figure 62. Time constants of voltage-dependent current activation. Time constants of current activation were plotted as function of voltage. Each point represents mean \pm s.e.m of five different oocytes. The time constants of activation were obtained by fitting the time course of current activation by a sum of two exponential functions (see text). **a)**, **b)** and **c)** present the time constants τ_1 and τ_2 at different exposure conditions: **a)** 2.3 mT, 16 hours continuous, **b)** 2.3 mT, 16 hours intermittent (5 min on/10 min off) and **c)** 1.0 mT, 16 hours intermittent (5 min on/10 min off).

No significant influence of ELF-EMF on the reversal potential of rCx46-mediated membrane current in oocytes.

Finally, the reversal potential V_{rev} of the rCx46-mediated membrane current was considered at different exposure conditions (Figure 63). The reversal potential is mainly determined by the expressed and conducting hemi-channels composed of rCx46, but also includes the contribution of all electrogenic transport systems. A field induced shift of the reversal potential would indicate a change of the intrinsic voltage sensor of the channel or by variation of the intracellular ion composition. No significant effect on the reversal potential of rCx46-mediated membrane current could be observed.

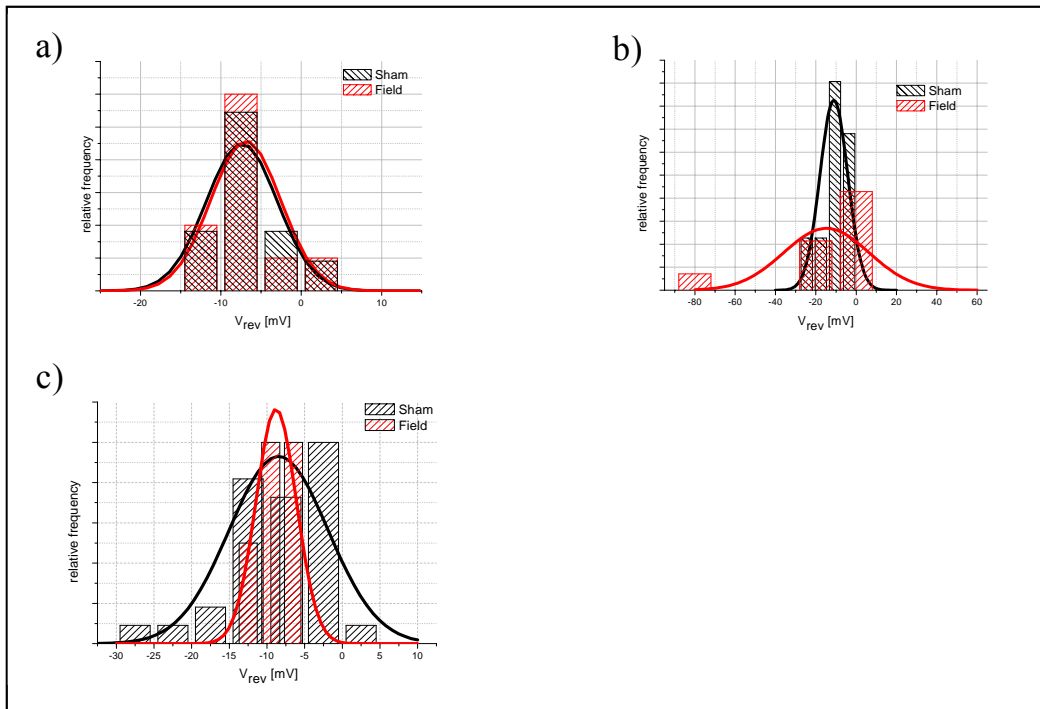


Figure 63. Relative frequency of reversal potential (V_{rev}) of conducting hemi-channels composed of rCx46 for different exposure conditions during an expression period of 16 h. The data were derived from the corresponding experiments given in Fig. 59. **a)** 1.0 mT, intermittent exposure: $n = 11$ for sham exposed and $n = 10$ for ELF-EMF exposed oocytes; **b)** 2.3 mT, permanent exposure: $n = 18$ for sham exposed and $n = 20$ for ELF-EMF exposed oocytes; **c)** 2.3 mT intermittent exposure: $n = 5$ for sham exposed and $n = 4$ for ELF-EMF exposed oocytes. Solid lines present the corresponding Gauss distributions using the parameters mean of relative frequency ($V_{rev, mean}$) and standard deviation (sd): **a)** $V_{rev, mean}(sham) = -6.9$ mV, $sd(sham) = 4.4$ mV, $V_{rev, mean}(field) = -7.4$ mV, $sd(field) = 4.4$ mV; **b)** $V_{rev, mean}(sham) = -11.1$ mV, $sd(sham) = 6.9$ mV, $V_{rev, mean}(field) = -14.8$ mV, $sd(field) = 2.1$ mV; **c)** $V_{rev, mean}(sham) = -8.8$ mV, $sd(sham) = 2.1$ mV, $V_{rev, mean}(field) = -8.5$ mV, $sd(field) = 0.7$ mV

A slight but not significant influence of ELF-EMF on the gating properties of hemi-channels expressed in *Xenopus* oocytes dependent on the external calcium concentration was observed.

The expression level of rCx46 in single were characterised by detailed biophysical analysis of corresponding voltage-jump current relaxation experiments. In parallel the gating by external Ca^{2+} concentration was characterised. A significant influence on the rCx46 mediated membrane conductance, the corresponding half-activation voltage ($V_{1/2}$) and the number of apparent equivalent gating charges (z) of the rCx46-hemi-channels in exposed and sham-exposed *Xenopus laevis* oocytes could not be observed for intermittently applied ELF-EMF at 50 Hz powerline signal (1.0 mT, 5 min on/10 min off) after an exposure time of 14 hours, 17 hours and 20 hours, respectively. Since it is known that external calcium significantly modulates the voltage dependent gating behaviour of expressed hemi-channels composed of rCx46, the experiments were repeated at various external calcium concentrations. The results indicate an influence by ELF-EMF exposure, but the differences are not significant (Figure 64). The membrane conductance and the gating parameters of exposed oocytes expressing rCx46 are smaller than those of sham exposed cells after an exposure time of 14 hours and 20 hours, respectively.

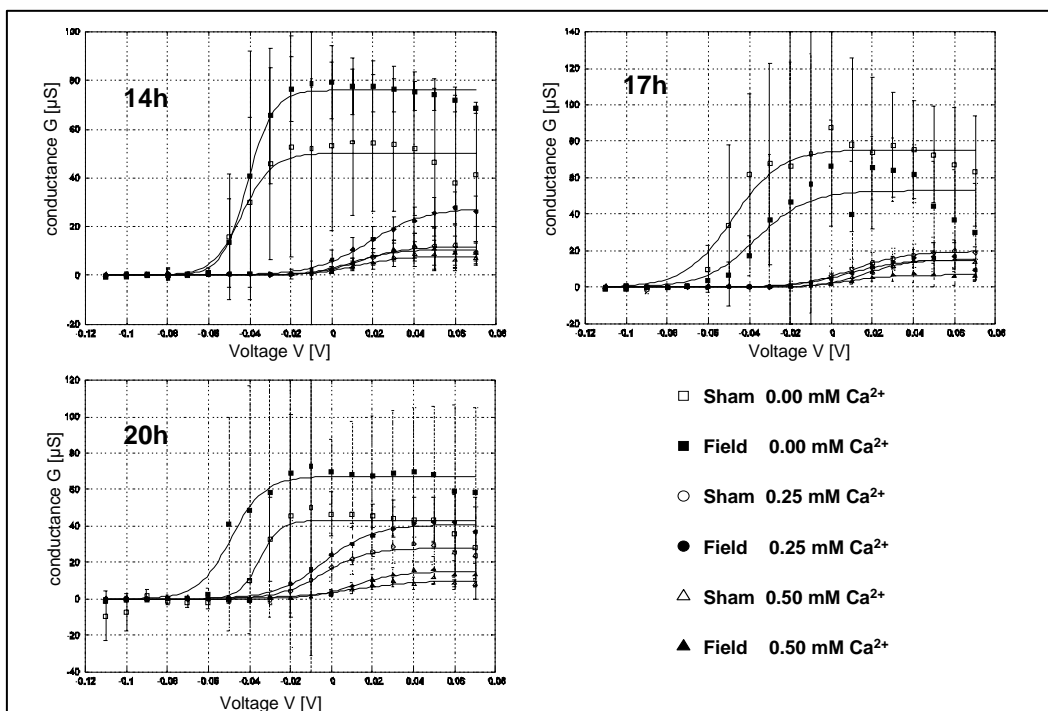


Figure 64. Conductance of hemi-channels composed of rCx46 expressed in oocytes after intermittent exposure (5 min on/10 min off) for 14 hours, 17 hours and 20 hours at 1.0 mT in the presence of 0.0 mM (n = 2-6), 0.25 mM (n = 2-4) and 0.5 mM (n = 2-5) Ca^{2+} in the bath. Closed symbols denote results of exposed oocytes and open symbols those of sham exposed oocytes.

ELF-EMF did not significantly affect the results of electrophysiological recordings of paired *Xenopus* oocytes.

The voltage-clamp experiments were repeated using paired oocytes. Paired oocytes expressing rCx46 form cell-to-cell channels (gap junctions) by head-to-head association of two hemi-channels which results in an increase of transjunctional conductance (G) between paired oocytes. Paired oocytes were intermittently ELF-EMF exposed (5 min on/10 min off) for 8 hours at 50 Hz powerline signal of 1.0 mT. The half-activation voltage ($V_{1/2}$) and the number of apparent equivalent gating charges (z) derived from the voltage-gating of junctional conductance of paired oocytes expressing rCx46 showed no significant change by ELF-EMF exposure (Figure 65). But the conductance of exposed paired oocytes is smaller than the conductance of sham exposed cell pairs. This finding is not significant on the basis of the 3 paired oocytes analysed so far.

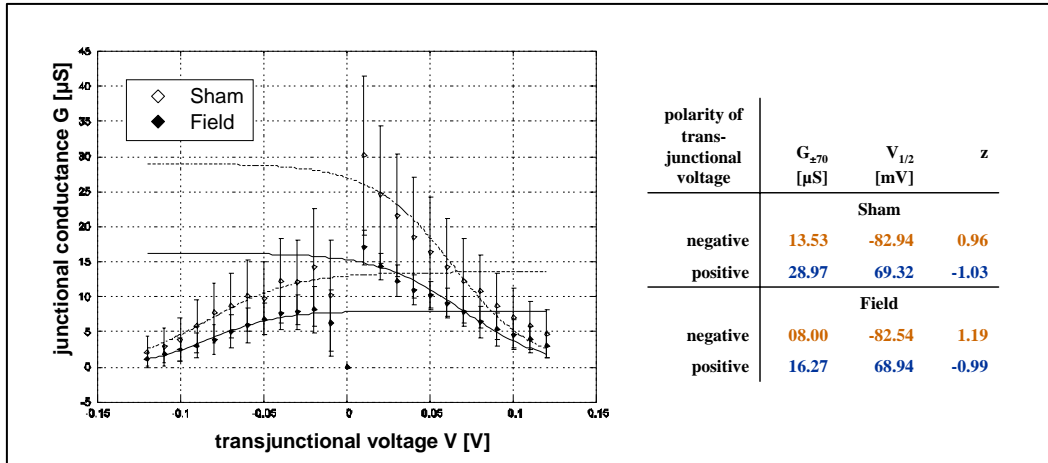


Figure 65. Mean junctional conductance (G) of paired oocytes expressing cell-to-cell channels composed of rCx46 as function of transjunctional voltage. The table summarizes the maximal conductance $G_{\pm 70} = G(V = \pm 70 \text{ mV})$ and the voltage-dependent gating parameters: the half-activation voltage ($V_{1/2}$) and number of apparent equivalent gating charges (z) of cell-to-cell channels after intermittent exposure (5 min on / 10 min off) for 8 hours at 1.0 mT, 50 Hz powerline (closed symbol: exposed cell pairs ($n = 3$); open symbol: sham exposed cell pairs ($n = 3$)). The parameter values were obtained by fitting the experimental data of G vs. V by a simple Boltzmann-distribution.

No significant influence of ELF-EMF on gap junctional coupling of rat granulosa cells was observed.

Gap junctional coupling by cell-to-cell channels of pairs of cultured granulosa cells was recorded after continuous exposure to ELF-EMF of 2.3 mT for 30 min. Figure 66a shows the maximal gap junctional conductance in the absence and presence of ELF-EMF exposure. The data were obtained as function of days in culture after passage, respectively. The corresponding mean gap junctional conductance of sham- and field-exposed cell all pairs is given in Figure 66b. No significant influence of ELF-EMF exposure on gap junctional coupling of rat granulosa cells was found.

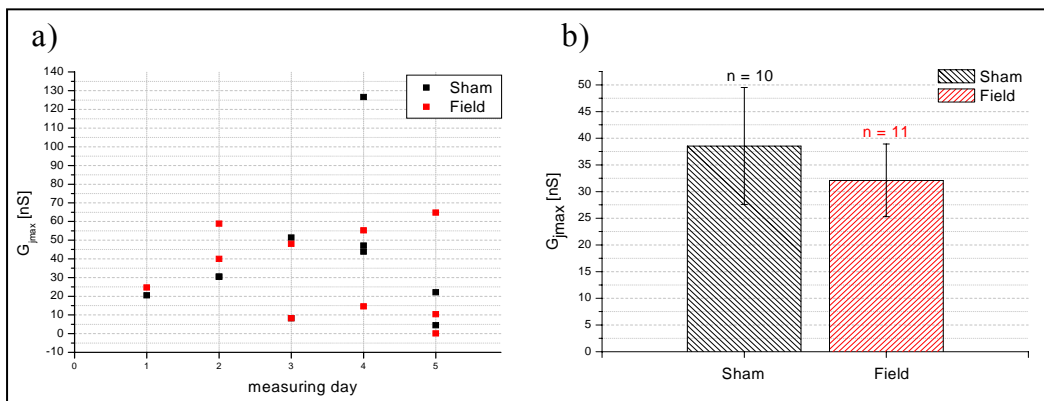


Figure 66. Gap junctional coupling of rat granulosa cell pairs as function of culture time in the presence and absence of ELF-EMF. **a.)** Maximal gap junctional conductance G_{jmax} of cultured pairs of granulosa cells in the absence (■, $n = 10$) and presence of ELF (■, $n = 11$) as function of time in culture. ELF-EMF was continuously applied with 2.3 mT for 30 min at room temperature, respectively. Measurements were performed by application of the double whole-cell patch clamp technique. **b.)** Mean \pm s.e.m. of gap junctional conductance measured at 1 to 5 days (see a)), in the absence ($n = 10$) and presence of ELF-EMF ($n = 11$). n denotes the number of different cell-pairs.

An effect of ELF-EMF on cytoplasmic free calcium of cultured human fibroblasts and granulosa cells of rats was not observed.

After exposure of fibroblasts for 5, 6, 7, 9, 10 and 11 hours to ELF-EMF $[Ca^{2+}]_i$ was recorded. Measurement of $[Ca^{2+}]_i$ was started 10 min after end of exposure and recorded up to 40 min under exposure –free incubation conditions. In Figure 67 $[Ca^{2+}]_i$ was followed after exposure for 11 h (Figure 67a) and 15h (Figure 67b). During the presented recording time no significant change of $[Ca^{2+}]_i$ was observed. The described experiments were repeated for a cultured granulosa cell line (not shown). The observed variability in the time course of $[Ca^{2+}]_i$ of some sham- and field exposed cells seems not to be significant. As in the case of fibroblasts a long-lasting influence of ELF-EMF on the time course and amplitude of $[Ca^{2+}]_i$ was not observed for cultured rat granulosa cells. For clearer presentation the results of $[Ca^{2+}]_i$ recorded for fibroblasts and rat granulosa cells are summarised in Table 9.

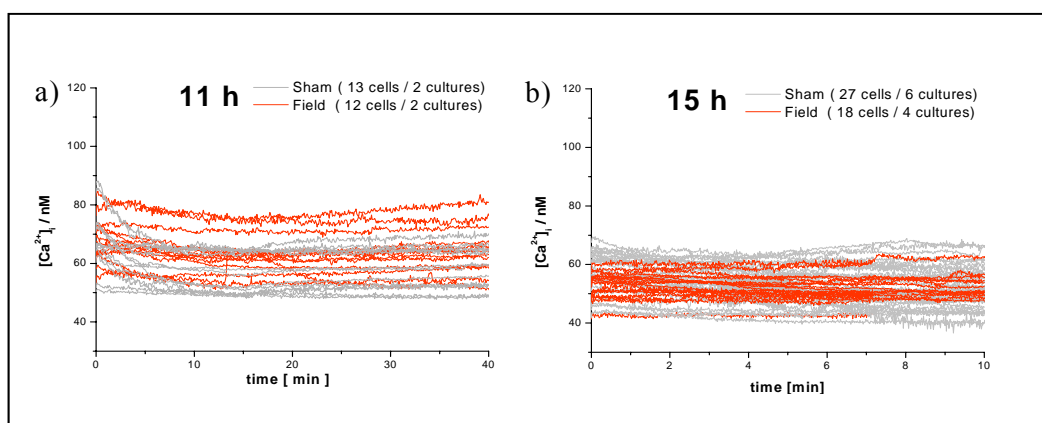


Figure 67. Time course of $[Ca^{2+}]_i$ in fibroblasts after ELF-EMF exposure at 50 Hz sinusoidal, 1.0 mT, intermittent (5 min on/10 min off) for **a)** 11 hours and **b)** 15 hours exposure time (grey curves denote sham- and red curves field-exposure)

Table 9. Summary of $[Ca^{2+}]_i$ data obtained on cultured fibroblasts and rat granulosa cells after ELF-EMF (5 min on/10 min off, sinusoidal 50 Hz, 1.0 mT) exposure

cell system	exposure time	7 h	9 h	11 h	15 h	17 h
Fibroblasts	sham	35 cells / 6 cultures	27 cells / 5 cultures	13 cells / 2 cultures	27 cells / 6 cultures	56 cells / 7 cultures
	field	37 cells / 6 cultures	15 cells / 3 cultures	12 cells / 2 cultures	18 cells / 4 cultures	14 cells / 3 cultures
		no ELF-EMF effect				
Granulosa	exposure time	4 h	5 h	6.5 h	7.75 h	
	sham	11 cells / 1 culture	54 cells / 5 cultures	60 cells / 5 cultures	51 cells / 3 cultures	
	field	19 cells / 2 cultures	57 Cells / 5 cultures	47 cells / 3 cultures	7 cells / culture	
		no ELF-EMF effect	no ELF-EMF effect	no ELF-EMF effect	no ELF-EMF effect	
ELF-EMF stimulation: 50 Hz, sinusoidal, 1 mT (5 min on / 10 min off)						

In a further series of experiments the cells were exposed to an additional stressor added to the bath after the end of ELF-EMF exposure. Figure 65 shows the time course of $[Ca^{2+}]_i$ of fibroblasts during an additional exposure to 200 μ M H_2O_2 in the bath. No significant effect on $[Ca^{2+}]_i$ could be found during a consecutive treatment by H_2O_2 . Application of another stress condition like cell- depolarisation by high external KCl (30 mM) also did not affect the time course and amplitude of $[Ca^{2+}]_i$ for ELF-EMF exposed cells (data not shown).

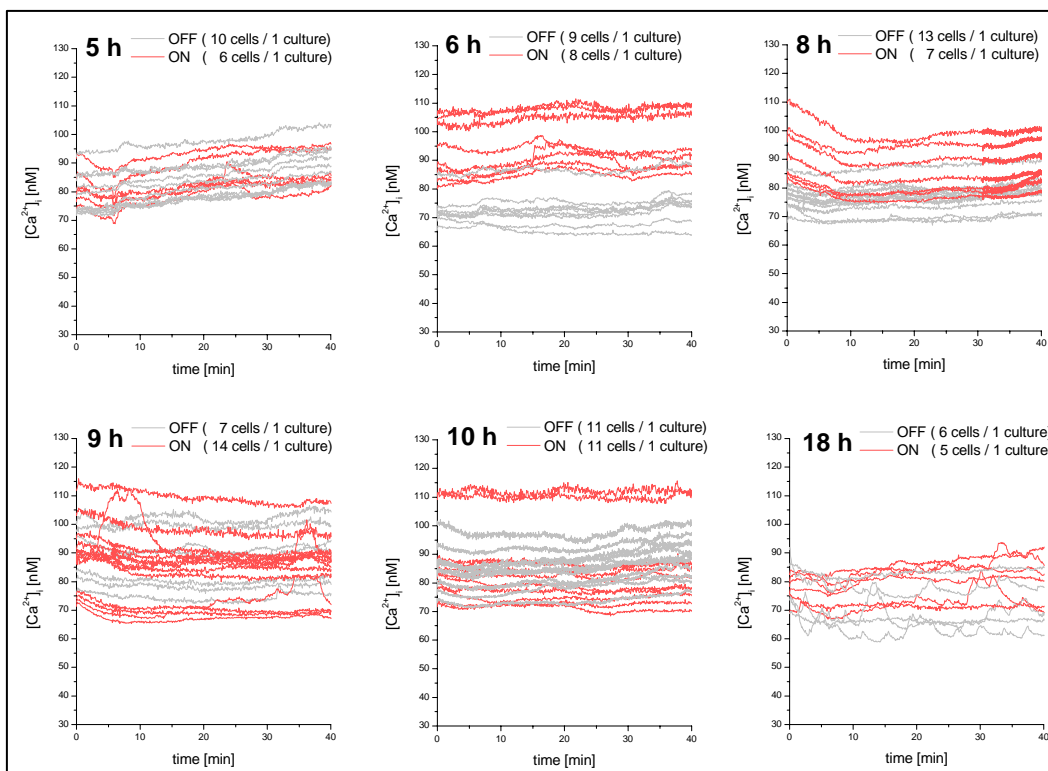


Figure 68. Time course of $[Ca^{2+}]_i$ in fibroblasts after end of ELF-EMF (5 min on/10 min off, 50 Hz sinusoidal, 1.0 mT) exposure for 5, 6, 8, 9, 10 and 18 hours which was followed by an addition of $200 \mu M H_2O_2$ to the bath for further 10 min (grey curves denote sham- and red curves field-exposure). For further details see text.

A summary of $[Ca^{2+}]_i$ measurements on fibroblasts and rat granulosa cells after application of ELF-EMF followed by addition of H_2O_2 to the bath is given in Table 10. $[Ca^{2+}]_i$ was recorded in the presence of $200 \mu M H_2O_2$.

Table 10. Summary of $[Ca^{2+}]_i$ data obtained on cultured fibroblasts and rat granulosa cells after ELF-EMF (5 min on/10 min off, sinusoidal 50 Hz, 1.0 mT) exposure followed by addition of H_2O_2 to the bath.

cell system	stimulation	exposure time	5 h	6 h	8 h	9 h	10 h	18 h
Fibroblasts	ELF-EMF and $200 \mu M H_2O_2$	sham	10 cells / 1 culture	9 cells / 1 culture	13 cells / 1 culture	7 cells / 1 culture	11 cells / 1 culture	6 cells / 1 culture
		field	6 cells / 1 culture	8 cells / 1 culture	7 cells / 1 culture	14 cells / 1 culture	11 cells / 1 culture	5 cells / 1 culture
			no ELF-EMF effect	no ELF-EMF effect	no ELF-EMF effect	no ELF-EMF effect	no ELF-EMF effect	no ELF-EMF effect
	ELF-EMF and 30 mM KCl	exposure time	6.5 h	7.5 h	8.5 h	9.5 h		
		sham	7 cells / 1 culture	7 cells / 1 culture	6 cells / 1 culture	7 cells / 1 culture		
		field	5 cells / 1 culture	5 cells / 1 culture	10 cells / 1 culture	8 cells / 1 culture		
		no ELF-EMF effect	no ELF-EMF effect	no ELF-EMF effect	no ELF-EMF effect			
Granulosa	ELF-EMF and $200 \mu M H_2O_2$	exposure time	5 h	6 h	7 h	8 h	18 h	
		sham	14 cells / 1 culture	14 cells / 1 culture	20 cells / 2 cultures	14 cells / 1 culture	14 cells / 1 culture	
		field	5 cells / 1 culture	5 cells / 1 culture	10 cells / 1 culture	8 cells / 1 culture	14 cells / 1 culture	
			no ELF-EMF effect	no ELF-EMF effect	no ELF-EMF effect	no ELF-EMF effect	no ELF-EMF effect	
ELF-EMF stimulation: 50 Hz, sinusoidal, 1 mT, 5 min on / 10 min off								

The volume regulatory response of granulosa cells appeared not to be influenced by ELF-EMF.

The volume regulatory response of cultured granulosa cells was studied after application of a hypotonic shock followed by a hypertonic shock. For clearer presentation for each experiment the volume change ($v(t)-v(t=0)$) of 10 cells was analysed as function of time and normalised to the maximal value v_{\max} , respectively. As exposure period again 18 h were selected, since after this exposure period rat granulosa cells show the maximal response on the genomic level. The volume regulatory behaviour of rat granulosa cells appears not to be influenced by ELF-EMF. In addition, there was no significant difference between exposed and sham exposed cells for hypotonic (Figure 69) as well as hypertonic conditions (not shown). The volume analysis was started 15 min after end of ELF-EMF exposure.

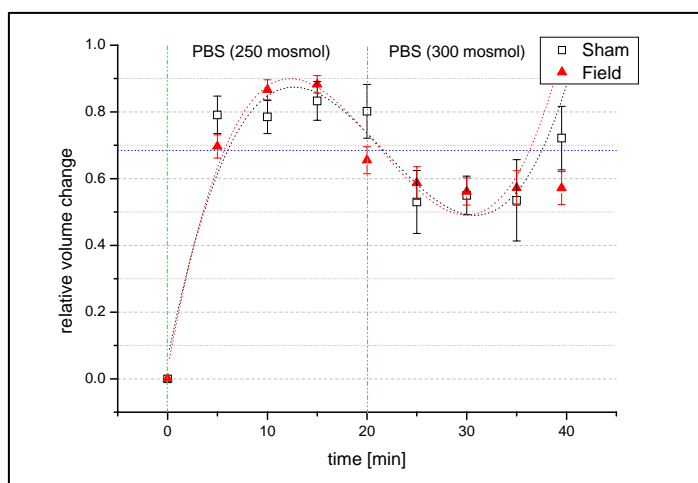


Figure 69. Relative volume change of granulosa cells (GFSHR-17) after addition of a hypotonic solution at $t = 0$. Prior to this treatment the cells were sham exposed ($n = 7$) or ELF-EMF exposed ($n = 24$) for 18 hours at 50 Hz, 1.0 mT, (5 min on/10 min off)). The mean \pm s.e.m. is given, respectively.

3.1.4.5 Whole-genome analysis of various cell lines exposed to ELF-EMF (Participant 12)

Altogether, 58 whole-genome analyses of 10 different cell lines (sham-exposed cells and control cells) were performed (Table 1). After primary data analysis, we only worked on genes which were reproducibly regulated in several experiments (see materials and methods) and which belonged to certain gene families (Table 11). We defined gene families which are potentially relevant for the cellular answer on EMF exposure: signal transduction, ion/electron transport, metabolism of energy/proteins, cell proliferation/apoptosis, immune answer/inflammation and extracellular matrix/ cytoskeleton. Each gene family was sub-divided in subgroups again, e.g. GTP proteins in the signal transduction family (Tables 11, 12). In a first step, we did not go into single genes, but simply counted genes up- or down-regulated in the different gene families. The total number of regulated genes in a certain gene family is not very meaningful, because the sizes of the gene families are of course very different. Therefore, the total numbers of genes on the human array belonging to a gene family are shown in the first column of Tables 11 and 12. Although a single gene might appear in different categories (e.g. all small G proteins are GTP binding proteins), the Tables give a good overview on what might happen in the cells after EMF exposure on the molecular level.

In human fibroblasts (Participant 3), a number of G proteins and calcium associated proteins involved in signal transduction seem to be strongly regulated. Genes involved in adhesion of cells and cytoskeletal genes appear strongly regulated in several hybridizations, although the variances in numbers between the experiments are high (Table 11).

The fibroblast experiments (Participant 3) were also assessed by bio-statistics (Participant 8: Dr. Remondini, Table 12): Mitochondrial and ribosomal genes appeared strongly regulated, also Ca-related genes, cell cycle, apoptosis, extracellular matrix, and the cytoskeleton. The overall number of significantly regulated genes is higher in the ELF-EMF treated fibroblasts than e.g. in endothelial cells

exposed to RF-EMF (Participant 6). This was expected, since the number of regulated genes in fibroblasts after ELF-EMF exposure is pretty uniform in the non-statistically evaluated gene numbers (compare Table 12 with Table 11). From the experiments with SY5Y human neuroblastoma cells (Participant 11) and mouse embryonic stem cells (Participant 4) it was not possible to extract bio-statistically significant data.

In detail, the following genes were extracted by bio-statistics so far:

Actin associated proteins (belong to cytoskeleton):

- Caldesmon (tropomyosin binding, actin binding. Activation of ERK MAP kinases lead to phosphorylation of caldesmon. Regulatory protein of the contractile apparatus): down-regulated (fibroblasts, participant 3).
- Gamma-actin: down-regulated (fibroblasts, Participant 3).
- "coactosin-like": down-regulated (fibroblasts, Participant 3).
- "actin-binding": down-regulated (fibroblasts, Participant 3).
- "procollagen-proline 2": down-regulated (fibroblasts, Participant 3).
- "actin modulating activity": up-regulated (fibroblasts, Participant 3).
- "actin-binding, calcium ion binding": down-regulated (fibroblasts, Participant 3).
- CD2-associated protein, actin binding: down-regulated (fibroblasts, Participant 3).
- Tropomodulin 3: actin binding down-regulated (fibroblasts, Participant 3).

Calcium (Ca²⁺)-associated proteins:

- protein phosphatase 4: down-regulated (fibroblasts, Participant 3).
- Thrombospondin (cell adhesion): down-regulated (fibroblasts, Participant 3).
- "EGF-containing fibulin-like..." (cell adhesion): down-regulated (fibroblasts, Participant 3).
- matrix metalloproteinase 2 MMP 2 (extracellular matrix, collagen metabolism): down-regulated
- follistatin (extracellular matrix, heparin binding): down-regulated (fibroblasts, Participant 3).
- SPARC (extracellular matrix, collagen binding): down-regulated (fibroblasts, Participant 3).
- ("myosin light polypeptide": up-regulated (fibroblasts, Participant 3).
- ("hypothetical protein": up-regulated (fibroblasts, Participant 3).

Extracellular matrix (ECM):

- thrombospondin (see Ca): down-regulated (fibroblasts, Participant 3).
- "EGF-containing..." (see Ca): down-regulated (fibroblasts, Participant 3).
- MMP2 (see Ca): down-regulated (fibroblasts, Participant 3).
- Connective tissue growth factor CTGF (cell adhesion, obviously not influenced by Ca): up-regulated (fibroblasts, Participant 3).
- Collagen XV (obviously not influenced by Ca): up-regulated (fibroblasts, Participant 3).
- Lysyl oxidase (also processed by bone morphogenetic protein 1 BMP1, obviously not influenced by Ca): up-regulated (fibroblasts, Participant 3).

Cytoskeleton (see also actin and calcium-associated proteins):

- "hypothetical protein": down-regulated (fibroblasts, Participant 3).
- "protein phosphatase 4, caldesmon): down-regulated (fibroblasts, Participant 3).
- "SH3 protein interacting with Nck": down-regulated (fibroblasts, Participant 3).
- "in kinesin complex": down-regulated (fibroblasts, Participant 3).

Ion transport:

- "potassium channel activity": down-regulated (fibroblasts, Participant 3).
- SLC12A5 KCl (potassium chloride) transporter: down-regulated (fibroblasts, Participant 3).
- SLC26A3 sulfate porter: down-regulated (fibroblasts, Participant 3).
- "ferric ion binding": down-regulated (fibroblasts, Participant 3).
- (ATP synthase, H⁺ transport): down-regulated (fibroblasts, Participant 3).
- ("H⁺ transporter): down-regulated (fibroblasts, Participant 3).
- "iron ion transport": down-regulated (fibroblasts, Participant 3).

Ribosomal proteins:

- 7 ribosomal proteins down-regulated, 3 ribosomal proteins up-regulated, 1 ribosomal protein up-regulated in profile nr.1, down-regulated in profile nr.2 (fibroblasts, Participant 3).

Table 11. Numbers of genes regulated within different gene families

Gene Family	total number of clones in Human Unigene RZPD-2	partner 3 fibroblasts Exp1 ELF up-regulated genes	partner 3 fibroblasts Exp2 ELF up-regulated genes	partner 3 fibroblasts Exp1 ELF down-regulated genes	partner 3 fibroblasts Exp2 ELF down-regulated genes	Gene "Superfamily"
Signal	2528	251	232	296	190	signal transduction
GTP	560	66	73	66	52	signal transduction
Small G	235	31	32	28	27	signal transduction
Jak	23	0	0	5	3	signal transduction
Rab	80	0	9	11	13	signal transduction
Ras	66	10	7	10	5	signal transduction
wnt	5	0	0	0	0	signal transduction
phosphatase	334	39	36	35	26	signal transduction
protein kinase	304	28	29	35	24	signal transduction
phospholipase	72	9	8	10	7	signal transduction
calcium	715	67	72	80	50	signal transduction
calmodulin	131	6	13	17	11	signal transduction
channel	348	31	25	36	22	ion/electron transport
voltage-gated	164	16	13	16	6	ion/electron transport
electron transport	423	52	52	57	37	ion/electron transport
ion transport	501	49	48	45	29	ion/electron transport
metaboli	1241	122	128	135	96	metabolism of energy/proteins
ATP	1234	113	112	157	82	metabolism of energy/proteins
mitochon	574	84	82	70	65	metabolism of energy/proteins
ribosom	254	47	48	32	39	metabolism of energy/proteins
translation	168	30	28	20	13	metabolism of energy/proteins
transcript	1991	201	190	228	136	metabolism of energy/proteins
cell cycle	478	46	52	54	43	cell proliferation/apoptosis/differentiation
apoptos	373	31	37	37	23	cell proliferation/apoptosis/differentiation
differentiat	177	14	21	22	11	cell proliferation/apoptosis/differentiation
immun	390	31	37	38	32	immune answer/inflammation/stress answer
inflamma	184	10	20	24	11	immune answer/inflammation/stress answer
stress	118	12	11	14	13	immune answer/inflammation/stress answer
peroxidase	32	6	5	4	6	immune answer/inflammation/stress answer
heat shock	188	4	7	5	3	immune answer/inflammation/stress answer
DNA repair	154	14	19	19	10	immune answer/inflammation/stress answer
early	8	2	2	0	2	immune answer/inflammation/stress answer
adhesion	573	46	49	53	43	extracellular matrix/cytoskeleton/adhesion
extracellular matrix	226	19	34	31	16	extracellular matrix/cytoskeleton/adhesion
cytosk	529	45	50	47	42	extracellular matrix/cytoskeleton/adhesion
junction	129	11	10	13	10	extracellular matrix/cytoskeleton/adhesion
actin	494	32	32	38	32	extracellular matrix/cytoskeleton/adhesion

Table 12. Numbers regulated genes in different expression profiling experiments (bio-statistical analysis by Dr. Remondini/Participant 8)

Gene Family	total number of clones in Human Unigene RZPD-2	partner 3 fibroblasts ELF up-regulated genes	partner 3 fibroblasts ELF down-regulated genes	Gene "Superfamily"
Signal	2528	0	12	signal transduction
GTP	560	0	2	signal transduction
Small G	235	0	1	signal transduction
Rab	80	0	1	signal transduction
Ras	66	0	1	signal transduction
phosphatase	334	1	2	signal transduction
protein kinase	304	0	1	signal transduction
calcium	715	2	6	signal transduction
calmodulin	131	0	1	signal transduction
channel	348	0	2	ion/electron transport
voltage-gated	164	0	1	ion/electron transport
ion transport	501	0	7	ion/electron transport
electron transport	423	0	3	ion/electron transport
metaboli	1241	0	4	metabolism of energy/proteins
ATP	1234	2	7	metabolism of energy/proteins
mitochon	574	0	5	metabolism of energy/proteins
ribosom	254	3	7	metabolism of energy/proteins
translation	168	3	0	metabolism of energy/proteins
transcript	1991	2	9	metabolism of energy/proteins
cell cycle	478	1	4	cell proliferation/apoptosis/differentiation
apoptos	373	0	4	cell proliferation/apoptosis/differentiation
differentiat	177	0	2	cell proliferation/apoptosis/differentiation
immun	390	0	2	immune answer/inflammation/stress answer
DNA repair	154	0	0	immune answer/inflammation/stress answer
inflamma	184	0	1	immune answer/inflammation/stress answer
adhesion	573	2	3	extracellular matrix/cytoskeleton/adhesion
extracellular matrix	226	2	5	extracellular matrix/cytoskeleton/adhesion
cytosk	529	1	6	extracellular matrix/cytoskeleton/adhesion
actin	494	1	4	extracellular matrix/cytoskeleton/adhesion
ijunction	129	0	0	extracellular matrix/cytoskeleton/adhesion

3.1.4.6 Summary (Participant 1)

Our data indicate that ELF-EMF may affect the gene and protein expression in various cell systems. This conclusion is based on the following findings:

- ELF-EMF at a flux density of about 2 mT up-regulated the expression of early genes, such as p21, c-jun and erg-1, in p53-deficient mouse embryonic stem cells, but not in healthy wild-type cells suggesting that the genetic background affects the responsiveness of the cells (see 3.1.4.1).
- ELF-EMF at a flux density of 2 mT up-regulated in neural progenitor cells the transcript levels of the GADD45 gene and down-regulated the transcript levels of the bax gene by which the apoptotic process may be modulated (see 3.1.3.1 and 3.1.4.1).
- ELF-EMF at a flux density of 0.8 mT up-regulated the expression of cardiac specific genes in cardiomyocytes derived from embryonic stem cells thus promoting cardiogenesis (see 3.1.4.3).
- ELF-EMF did not affect the expression of neuronal genes in neuroblastoma cells (SY5Y) such as nAChRs, D β H, Phox2a and Phox2b, either at mRNA or protein level (see 3.1.4.2).
- ELF-EMF did not affect either the expression level of conducting hemi-channels composed of rCx46, nor their gating properties by voltage, pH, Ca²⁺ in *Xenopus laevis* oocytes (see 3.1.4.4).
- ELF-EMF appeared to regulate the expression of a series of genes and proteins in human fibroblasts such as mitochondrial and ribosomal genes as well as Ca-, cell cycle-, apoptosis-, extracellular matrix-, and cytoskeleton-related genes, although it must be considered that the variances observed between the various experiments was high (see 3.1.4.5).